GRID RESILIENCY ISSUES WITH A HYBRID SOLAR- BATTERY SYSTEM

A THESIS SUBMITTED
TO THE BOARD OF GRADUATE PROGRAMS
OF
MIDDLE EAST TECHNICAL UNIVERSITY, NORTHERN CYPRUS CAMPUS

BY

MOAZ ZIA

IN PARTIAL FULFILLMENT OF THE REQUIREMENTS
FOR
THE DEGREE OF MASTER OF SCIENCE
IN ELECTRICAL AND ELECTRONICS ENGINEERING PROGRAM

AUGUST 2021

Approval of the Board of Graduate Programs

_____

Prof. Dr. Oğuz Solyali

Chairperson

I certify that this thesis satisfies all the requirements as a thesis for the degree of Master of Science

_____

Assoc. Prof. Dr. Murat Fahrioğlu

Program Coordinator

This is to certify that we have read this thesis and that in our opinion it is fully adequate, in scope and quality, as a thesis for the degree of Master of Science.

_____

Assoc. Prof. Dr. Murat Fahrioğlu

Supervisor

Examining Committee Members

Asst. Prof. Dr. Mehmet Şenol	Electrical and Electronics Engineering Program CIU _____
Assoc. Prof. Dr. Murat Fahrioğlu	Electrical and Electronics Engineering Program METU NCC _____
Asst. Prof. Dr. Canraş Batunlu	Electrical and Electronics Engineering Program METU NCC _____

I hereby declare that all information in this document has been obtained and presented in accordance with academic rules and ethical conduct. I also declare that, as required by these rules and conduct, I have fully cited and referenced all material and results that are not original to this work.

Name, Last name: MOAZ ZIA

Signature :

ABSTRACT

GRID RESILIENCY ISSUES WITH A HYBRID SOLAR-BATTERY SYSTEM

Zia, Moaz
Master of Science, Electrical and Electronics Engineering Program
Supervisor: Assoc. Prof. Dr. Murat Fahrioğlu

August 2021, 58 pages

Harmonics are one of the main power quality issues which needs to be addressed while designing a microgrid. If harmonics are present in the system, they can cause the load to malfunction and damage. With increasing number of non-linear loads and integration of distributed generators (DG) into the power system, harmonic mitigation is of paramount importance. There is a lot of work available in literature which deduce the benefits of integrating battery into the microgrid to improve renewable energy source (RES) fraction but very few studies go over the effect of battery on the power quality of the system. This study presents a detailed analysis of the effect of battery integration on the harmonics of the interfacing converter (IFC) output of PV microgrid. A resonant converter (RSC) controller with a voltage controller is used for the IFC control. For a comparative analysis, the THD for the PV-battery microgrid is compared with the THD of a standalone PV system. The simulation shows that upon integrating the battery the THD of the unfiltered converter output voltage increases from 33.89% to 40.75%. But after filtration of the higher order harmonics, the THD for PV-battery microgrid is 1.89% whereas for the PV microgrid is 2.34%. This shows that the integration of battery increases the high order harmonics due to unbalance in DC-link voltage during switching of charging states of the battery but complements the IFC control to reduce the lower order harmonics. Hence after filtration, the THD of the system is less if there is battery integration. The unbalance generated by battery is also under the acceptable IEEE limits. The impact of battery on the stability of the DC-link and minimizing the

reactive power at the output is also discussed. Integration of battery helps in keeping the DC-link voltage more stable leading to lesser amount of reactive power at the output. This is a big advantage of using batteries especially in a weak grid where IFC needs to compensate large amount of reactive power.

Keywords: Harmonics, Distributed Generators, Interfacing Converters, Resonant Converter, Battery Integration

ÖZ

HİBRİT GÜNEŞ PİLİ - AKÜ SİSTEMİ İLE ŞEBEKE ESNEKLİĞİ SORUNLARI

Zia, Moaz
Yüksek Lisans, Elektrik ve Elektronik Mühendisliği
Tez Yöneticisi: Doç. Dr. Murat Fahrioğlu

Ağustos 2021, 58 Sayfa

“Harmonik”ler mikro-şebeke dizayn ederken dikkate alınması gereken ana problemlerden birisidir. Sistemde harmonikler bulunurlarsa yükün işlev bozukluğuna uğrayıp zarar görmesine neden olabilir. Doğrusal olmayan yüklerin sayısındaki ve dağıtılmış jeneratör (DJ) entegrasyonundaki artıştan dolayı harmoniklerin hafifletilmesi yüksek önem arz etmektedir. Yenilenebilir enerji kaynağı (YEK) bölümünü geliştirmek için mikro-şebekeye batarya entegre etmenin faydaları konusunda literatürde halihazırda eserler bulunmakta fakat çok azı bataryanın güç kalitesindeki etkileri üzerinde durmakta. Bu eser PV mikro-şebekesinin arayüz (ARA) harmonikleriklerine batarya entegrasyonunun etkilerini detaylı bir analizle sunmaktadır, ARA kontrolüne voltajla kontrol edilen rezonans dönüştürücü (RED) kontrolünde. Karşılaştırmalı analiz için, PV bataryalı mikro-şebeke ve sade bir mikro-şebekenin toplam harmonik distorsiyonu (THD) karşılaştırılır. Simülasyon batarya entegre edildikten sonra filtrelenmemiş dönüştürücü üretim voltajında %33,89 dan %40,75 e artış göstermiştir. Fakat yüksek düzen harmoniklerinin filtrelenmesinden sonra PV bataryalı %1,89, sade PV mikro-şebekeleri %2,34 olarak ölçülmüştür. Bu, bataryanın entegrasyonunun DC-link voltajının bataryanın şarj dönemlerindeki değişim süresindeki dengesizliğinden ötürü yüksek düzen harmokinleri arttırırken aynı zamanda ARA kontrollerine yardımcı olup düşük düzen harmoniklerini azaltmaktadır. Böylelikle, eğer batarya entegrasyonu varsa sistemde THD daha azdır. Bataryanın oluşturduğu dengesizlikler IEEE kabul edilebilir limitleri arasındadır. DC-linkin stabile olmasında bataryanın etkisi ve üretimdeki reaksiyon gücünü minimuma

indirme konuları da tartışılmıştır. Bataryanın entegrasyonu DC-link voltajını stabil tutmaya yardımcı olup üretimde daha az reaksiyon gücü olmasını sağlar ve bu ARA kontrollerinin yüksek miktarda reaksiyon enerjisini telafi etmesi gereken zayıf şebekelerde özellikle olmak üzere kullanılabilecek büyük bir avantaj.

Anahtar kelimeler: Harmonikler, dağıtılmış jeneratör, arayüz, rezonans dönüştürücü, batarya entegrasyonu

I dedicate this dissertation to Almighty Allah, the most Beneficent and Merciful, for allowing me to complete this study and obtain positive results, my parents (Dr. Arshad Zia and Qudsia Sabri) and siblings (Zain Zia and Hassan Zia) for their prayers and support.

ACKNOWLEDGEMENT

I came to Middle East Technical University, Northern Cyprus Campus (METU NCC) in 2014 when I was 17 years old. After graduating from bachelors with honors, I was awarded graduate assistant assistantship to continue my master studies. Now that my master studies is coming to an end with this thesis, I would like to mention people which helped me during this period.

Firstly, I would like to thank Almighty Allah for allowing me this opportunity to conduct my master studies in such a prestigious university and giving me the strength to complete the studies with high grades.

Secondly, I would like to mention Asst. Prof. Dr. Murat Fahrioğlu and Asst. Prof. Dr. Canraş Batunlu who were not only a guide for me for the thesis and courses, but he also taught me a lot about the professionalism and how to carry myself in academic affairs. They helped me throughout the thesis to make sure that my work was backed up by literature and was of highest quality.

Thirdly, I would like to thank all of the EEE faculty members in METU NCC and professors from other departments which helped me during my studies.

I would like to acknowledge my parents and my brothers. My parents worked hard during their life to make sure I have the highest quality education possible. I would like to thank my elder brother Zain Zia, who stayed with my parents while I was away for masters and gave me comfort that someone was there to stay with my parents. Also, my brother Hassan Zia who was source of motivation and giving me sense of competition. Both are the best role models a brother can have.

I would like specifically thank Syed Muhammad Messam Raza. I met him in 2016. Ever since then he has been a constant emotional support helping me with studies and my personal life. Also, I would like to thank Ahmed Zarrar who I met during the start of my master studies. Although, I have known him for only 3 years but it’s a friendship

which I am certain will last for a long time. These two people made the past 3 years of my life, one of the most wonderful experience I could have.

Lastly, I would like to thank all people who became my family at METU NCC and helped me to go through this period with ease. Sebil Demir, Haseeb Maila, Ammar Shazy, Baboo Iftikhar, Anjum Sohail, Ali Babloo, Essam Bibi, Inam Khilari, Uncle Seiman, Musadiq Kabotar, Shaye Paracha, Bassam Abdulwahab, Muhammad Alsaleh and Burak Can Baytop are some of the few which have made METU NCC my second home.

TABLE OF CONTENTS

LIST OF TABLES

TABLES

LIST OF FIGURES

FIGURES

LIST OF ABBREVIATIONS

ABBREVIATIONS

RES	Renewable Energy Sources
DG	Distributed Generators
IFC	Interfacing Converter
ESS	Energy Storage Systems
LCOE	Localized Cost of Energy
MPPT	Maximum Powerpoint Tracker
CFL	Compact Fluorescent Lamp
ASD	Adjustable Speed Drive
THD	Total Haromic Distortion
VCM	Voltage Control Method
CCM	Current Control Method
LVRT	Low Voltage Ridethrough
EMT	Electromagnetic Transient
RSC	Resonant Converter
DB	Deadbeat Controller
RC	Repetitive Controller
PCC	Point of Common Coupling
NPC	Neutral Point Clamped

CHAPTER 1

INTRODUCTION

Industrial Revolution took place from 1760 to 1840. It ushered in a new era that saw the shifting of economies from agricultural to industrial. Industries were built all over, and machines replaced human work. However, energy was required in order to power those industries. Coal was the most abundant natural resource available whose energy could be harnessed. From that period onward, there was an unprecedented increase in the use of fossil fuels for the production of electricity. At that time, people did not know the consequences of their actions. But in the past half a century, people have debated whether our excessive use of fossil fuels is damaging the environment or not. Most people shunned that idea and titled ‘global warming’ as a hoax. But in the past decade or two, there has been too much evidence advocating the presence of global warming.

Now that there was substantial evidence that global warming is not a myth but something which can be catastrophic for us if we do not do anything to change our ways, different treaties and pacts were signed which set certain goals for countries involved to meet and held them responsible if did not meet those demands. Goals of these pacts were to move towards a more sustainable future. Kyoto protocol and the Paris agreement are examples of such pacts. Apart from pacts, there was a rise in research to find any alternative energy sources available that can replace the conventional energy sources. In this time, renewable energy sources (RES) such as PV and Wind energy started catching people’s eyes and were viewed as the solution to guide us towards a sustainable future.

Much research was then started in order to make PV and Wind energy an attractive energy production option for energy markets. However, PV and Wind have a significant flaw which is the dispatchability. Conventional resource generators like Coal Power Plants are kept running 24/7, and when energy is required, it is dispatched quickly hence they are called spinning reserves. With PV and Wind, there is no

certainty that when energy is required, they would produce power to meet the demand. Maybe there is shading due to clouds that reduce the PV plant's efficiency, or it is after sunset causing no energy production in PV plants, or the wind is not sufficient to drive the generators in a Wind Turbine. Due to this reason, spinning reserves are needed in the grid despite the presence of RES.

One solution to this problem is connecting the microgrid to the main grid. If there is RES energy production, the power is first fed into the grid and then loaded from the grid. An issue that comes up with this approach is that penetration of RES with the grid effect the power quality of the power systems. Because the power production from RES varies, an interfacing converter (IFC) is required to maintain constant power before feeding it into the grid. The power conversion in IFC usually leads to power quality issues in the grid. As the penetration of RES increases, a lot of work is being done to mitigate the power quality issues and bring it to the standard set by IEEE.

Another solution to this problem is Energy Storage Systems (ESS). Using ESS, the excess power from renewable can be stored and when it is required, it can be dispatched accordingly without depending on the spinning reserves. Examples of ESS are Pumped Hydro, Flywheels, Super Capacitors, and Batteries. Decades ago, this was not a feasible solution because of the general cost of the ESS systems. However, in recent times the overall cost of ESS of the systems has gone down along with installing renewable energy sources. So, the overall Localized Cost of Energy (LCOE) has gone down, making them an attractive option for energy markets.

Different power quality issues which come up are Current Imbalance, Voltage Imbalance, Frequency Variations, and Harmonics. Frequency Imbalance is dealt with during the power conversion process. Voltage Imbalance and Harmonics are the most important as they require a separate filter (active or passive) to fix. A passive filter is referred to a filter composed of physical elements like an Inductor or a Capacitor. In contrast, an Active Filter is composed of a control system that controls the IFC in order to improve the power quality. In recent times, different filtering techniques have been implemented (active and passive) to improve power quality. Active filtering is usually

preferred as it is usually a cheaper option compared to passive filtering as no bulky equipment is required. Active filters are usually designed to filter out the lower order harmonics, and passive filters are used to remove the high order harmonics.

1.2. Motivation

Electricity is one of our fundamental needs and our demand increasing every year. Most of the electricity we produce now is through fossil fuels. Due to worry about global warming, countries started investing in RES to reduce CO_2 emissions. Recently, the cost of installing RES into the system was a reason that energy suppliers were reluctant to install them. Energy market operators had to give incentives to energy suppliers, so they produce energy using RES. Nevertheless, in recent time, due to advancements in technology, the LCOE has decreased considerably. However, even with lower LCOE, due to inertia problems, a considerable number of spinning reserves are still required to ensure the smooth running of a power system. So even if we increase the efficiency of RES to the same levels as fossil fuels, there would still be a need for spinning reserves that need to be kept running 24/7. A solution to this problem is the integration of ESS into the system. ESS will enable us to store the excess energy, and when RES cannot supply the load, it can be satisfied using ESS. But to integrate ESS, the IFC controller needs to be designed properly to maximize the power quality. If the inclusion of an ESS into microgrids makes it cost-effective, it will lead to the LCOE of RES going down, making it a more attractive option for energy producers that take part in energy markets. It will be a huge step forward towards a more sustainable future. For a country like Cyprus with massive solar potential, ESS integration can significantly help in energy crises without effecting the environment.

1.3. Objective of Study

The main objective of this study is to model a PV-Battery-Grid microgrid, observe the power quality issues and improve the power quality. The PV and demand are modeled on Excel and MATLAB according to our campus, which is located in Kalkanli, Northern Cyprus. Currently, in the literature, there is a lot of research available

regarding active filters and passive filters being used to improve the power quality of the microgrids. However, they usually do not have an ESS integration. The studies available in the literature usually go over the storage benefits of ESS but they do not go over the power conditioning effects of batteries. This study presents a step-by-step design for a PV-Battery-Grid system. Design each subsystem from Maximum Power Point Tracker (MPPT) to the active filter design is explained in detail, and the results are verified based on IEEE standards for power quality which are discussed in detail in the literature. Active filter coupled with a passive filter is used to tackle the Harmonics and Voltage Unbalance issues, one of the main power quality issues that arise in such microgrids.

Chapter 2 will cover the literature research, which encompasses all topics from the type of Microgrid topologies beings used to different battery management strategies used. Chapter 3 will cover the Theory and Methodology used in building the system. Chapter 4 will contain the results and discussion and the Chapter 5 will conclude the study.

CHAPTER 2

LITERATURE REVIEW

This section covers the literature review that was done in order to conduct this research. The study of power quality mitigation is becoming a very popular topic for scholars because of the increasing penetration of non-linear loads and the integration of DG into the grid. Power quality issues can occur anywhere from Data Centers to Electric Vehicles to Distribution Systems. This literature review will be focused on the power quality issues in power systems.

Due to the increase in the use of non-linear loads, there has been an increase in the power quality issues in the grid. Loads like fluorescent lamps (CFL) and adjustable speed drives (ASD) have non-linear load profiles. Their consumption of energy varies with time due to which power quality issues occur. Similarly, with the integration of RES into the microgrid, an IFC is required to ensure constant delivery of power to the load. As RES is changing with time, IFCs can also cause power quality issues.

2.1 Power Quality issues

There are different power quality issues that can occur in a power system. These issues can be in the form of voltage imbalance, harmonics, frequency variations, and transients. Frequency variations can quickly be addressed using the control of the interfacing converter (IFC's), but other power quality issues present a deeper challenge.

2.1.1 Voltage Unbalance

Voltage unbalance is a power quality issue that presented itself even before the integration of RES. Previously, they were caused due to unbalanced loads and grid faults. When there is a number of single-phase loads in a three-phase system, it can lead to unbalance voltages [1]. These single-phase loads can be large commercial setups, electric power systems in rural areas, railroad systems, and electric transit

systems. If the design of the power supply to such loads is not done correctly, it may cause voltage unbalances in the grid. For example, in large commercial setups, there are a large number of single-phase loads. These loads need to be divided evenly among the three-phase incoming supply. In the case of their uneven distribution, it may cause stress on a particular phase causing voltage imbalances in the grid even though the power supplied is balanced [2]. Figure 2.1 shows an example of an unbalanced 3-phase voltage.

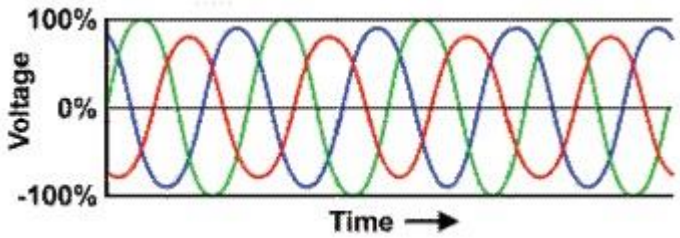

Figure 2.1. Voltage unbalance in 3-phase systems

Besides the loads, voltage unbalances are also causes due to various electrical equipment used in the power distribution. In long transmission lines, there may be impedance differences between them, causing voltage unbalance. Usually, impedance unbalance is the leading cause of voltage unbalance. Faulty capacitive banks, uneven transformer impedances, open contacts, or loose contacts in electrical equipment can cause imbalances [3].

Apart from the reasons mentioned above, there are new causes of voltage imbalances. Nowadays, a lot of “Energy saving schemes” are being implemented to save power. Although they indeed save power, but they are usually non-linear loads. Instead of constant energy consumption, they consume power “irregularly” to save power, but due to this uneven power consumption, they cause voltage unbalances. Also, they usually have non-linear electric components like diodes which draw current non-linearly [4]. Modern speed drives like ASD are an example of such schemes which cause voltage imbalances.

2.1.1.1 Effects of Voltage Imbalance

Voltage unbalances are not desired as they affect the power system in general and the equipment present in the power system. The power system is a very sensitive system. Even a minor disturbance can have a big effect on the whole system. When a voltage unbalance occurs, it can cause significant current surges or overshoots even if it is small. These currents in turn increase the power loss. This power loss causes increased temperature which can cause adverse effects like melting of transmission lines or melting of other equipment. This can lead to short circuit faults that can cause the whole system to break down if not dealt with quickly. Apart from that, these current surges can cause the loads to malfunction and increase their degradation and, in severe cases, can damage the loads permanently.

2.1.2 Harmonics

In the simplest definition, harmonics are signals whose frequencies are multiples of the fundamental frequency. These signals can be produced when the signal passes through a circuit that has non-linear voltage-current characteristics [5]. So after passing through such a circuit, these harmonics get superimposed on the output signals causing the output signal shape to be distorted (non-sinusoidal). Harmonic signals are an issue for all different engineering fields, and there are various studies being carried on mitigating them.

But in case of power systems and power electronics, they pose a big problem. Most of the renewable energy sources are non-linear. The power output depends on various variables that can change during the course of energy production, giving rise to varying power output. This power output is regulated using power converters that have non-linear voltage-current characteristics. This non-linearity then in turn gives rise to harmonics. Different filters like LCL filters are used to reduce the harmonics but they are usually effective in mitigating the high order harmonics and are expensive to implement. So IFC control is used to adjust the gate pulses of the converter to not only deliver constant output but to improve the harmonic characteristics.

2.1.2.1 Effects of Harmonics on a Power System

Harmonics can be very harmful to a power system. Harmonics affect the power effect the overall power factor of the system. The apparent power of the system under harmonics is shown in equation 2.1.

$$S = \sqrt{P^2 + Q^2 + D^2} \tag{2.1}$$

Where 'P' is the active power, 'Q' is the reactive power and 'D' is called the distortion power. Just from the equation 2.1. it is clear that under harmonics, the system must produce more power while the active power at the fundamental frequency does not change. This causes the overall power factor of the system to drop and reduces the efficiency of the system [4]. Also, due to the increase in the apparent power, the current drawn increases. This increase in current leads to more conductive losses. In some equipment such as capacitor banks, it causes resonances that lead to power losses in those components and in worst scenarios, cause them to malfunction. Some equipment which are highly susceptible to harmonics are digital circuits, transformers, motors, generators, circuit breakers and fuses. Due to these reasons, specific criteria are set by IEEE under which all power systems should operate, shown in table 2.1 [6].

Table 2.1. Standards set by IEEE for THD

Power System Voltage Level	Low Voltage 2.3-69 kV	Medium Voltage 69-138 kV	High Voltage >138 kV
THD level	5%	2.5%	1%

2.2. Power Quality Improvement using control of interfacing converters

IFC is used for Bi-Directional power transfer. They can be AC/DC, AC/AC, DC/AC or DC/DC converters. The choice of using the IFC is dependant on the voltage input and output. Previously, there was a need for only primary control responsible for controlling the output voltage and current based on the reference set. Voltage control method (VCM) or current control method (CCM) are examples of different primary control structures which can be implemented. Hybrid control methods incorporate both

CCM and VCM for IFC control. Due to an increase in power quality issues, IFC's job is not only to provide the desired voltage and current at the output but also to ensure the power quality under the set standards. This gave rise to the design of complex IFC control algorithms.

2.2.1 Unbalance Voltage Improvement using IFC control

In order to counter the voltage imbalance, there must be an external injection of power into the system to maintain the power supplied to the grid. However, due to external injection of power, there may be some power oscillations or over-currents in the system. Some studies do not take these effects into considerations, while some of them do. Studies by Nejabatkhah et al. [7] and Camacho et al. [8] are examples of studies that use the external power injection into the grid to compensate for the voltage sag without considering the power oscillation.

Lee et al. [9] use the Low-Voltage Ride Through technique (LVRT) for voltage unbalance compensation and control the power oscillation effect. In this method, active power, as well as reactive power, are injected into the system to support the grid during voltage unbalance. It is important to note that the power injection is during both positive and negative sequences but as there is a predefined current constraint for the converter, the output current value never goes above the constraint, and there are no power oscillations.

During voltage sags, there is an over-current being produced, which can make the grid vulnerable. A study by Miret et al. [10] improves the power quality during voltage sags by limiting the peak currents during the voltage sag. In their controller, first, the unbalance factor is calculated and stored in the lookup table. Corresponding to the unbalance factor, the controlling parameters for the reference current are calculated such that the minimum peak current at the output is obtained and stored in the lookup table. So during operation when voltage sag is detected during operation, the unbalance factor is first calculated and corresponding control parameters are obtained from the lookup table. The experimental results were really promising, and peak currents were considerably reduced using their control strategy.

A study by Camacho et al. [11] tackled the voltage sag issue using a reference generator. They provide a control strategy based on two objectives, to maximize the power transfer and to control the over currents during the fault. This method is really effective as it can be applied to any power converter from high power to low power. Similar to the study above, the main contribution is the calculations of the control parameters for the injection currents. But compared to other methods, it also takes the power output into account to make sure that the power transfer is maximized.

A study by Lu et al. [12] proposed two strategies to mitigate the voltage unbalance caused by load disturbances. Their study is based on the fact that active power oscillations and the voltage unbalance are related. In the first method, the IFC is controlled in such a way that the active power oscillations are completely cancelled, leading to a reduction of negative sequence voltage to a certain level. However, as the voltage unbalance is being mitigated indirectly by reducing power oscillations, the level of voltage unbalance mitigation is uncertain. In the second method, the negative sequence voltage is completely mitigated by comparing it to a set reference point, therefore, minimizing the power oscillations to a certain level. They mention that depending on the grid infrastructure, one of the two methods can be chosen.

A study by Chaudary et al. [13] proposes a technique to mitigate the voltage unbalance and power oscillations caused due to wind turbines. To mitigate the negative sequence voltage, they used the electromagnetic transient (EMT) model. The negative sequence current injection is derived using the EMT model, and based on the error with the reference, the PWM signals are generated. Their results show that the proposed control strategies reduce the negative sequence voltages and reduce the active power oscillations.

2.2.2 Harmonics Mitigation Using IFC control:

The presence of harmonics can be adverse to the grid. It can cause losses and resonances. A study by Salles et al. [14] goes over the impact which harmonics have on the grid. Their study goes over on how the harmonics can have adverse effects on the grid as well as various loads. Harmonics can be removed using active and passive

filters. Passive filters use electrical components like inductors and capacitors to remove frequency. These filters are usually low pass filters that have high impedance at high frequencies, so high order harmonics are removed. These filters are usually expensive, so lower-order harmonic mitigation using passive filters is not preferred. Hence to remove lower order harmonics, IFC control is preferred. There are different controllers like resonant (RSC), deadbeat (DB), and repetitive controller (RC), which can be used in IFC control to remove harmonics.

An ideal RSC has infinite gain at the resonant frequency, so by pairing multiple RSC in parallel and setting the resonant frequency as the frequency which needs to be eliminated, specific harmonics can be targeted as shown in the figure 2.2 [15]. All RSC-based active filters have a similar concept. The error signal for the current command is obtained by comparing it to a reference and sent to the RSC to obtain the voltage command for the PWM generation. The difference between the studies available in the literature is how they generate the current command and alter the voltage command generated to increase the efficiency of the active filter.

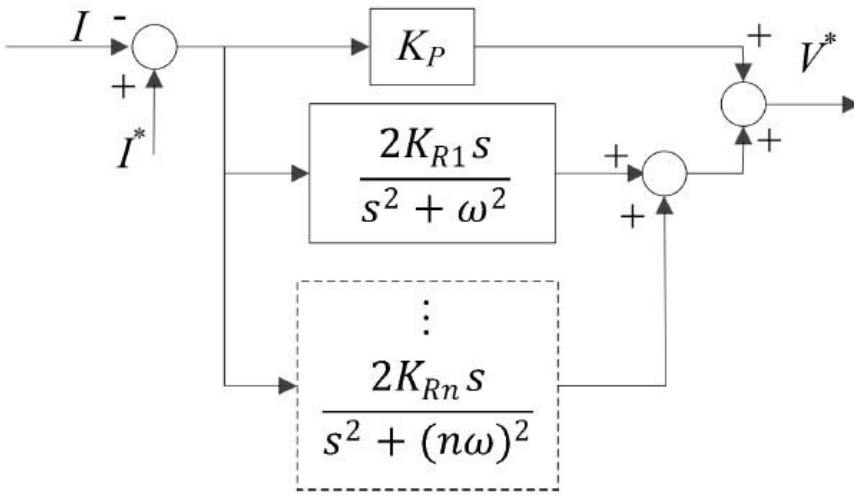

Figure 2.2. Parallel RSC connection

A study by Xin et al. [16] uses an RSC to ensure the injection of high quality of power even under voltage distortions. It uses a proportional controller along with an RSC to maintain power quality. This method makes sure that the harmonics are produced at

the inverter side and the harmonics produced are compensated using a capacitor. As the information about the harmonics is already available from the RSC, the capacitor can be adjusted to compensate for the harmonics. A total harmonic distortion of 2.8% was achieved while maintaining the injected current distortion at 0.6% which falls under the grid requirement. A study by De et al. [17] also used RSC to improve power quality issues, but they implemented it using a three-phase four-wire high-frequency link power converter along with a novel control strategy. Their model was able to reduce the THD from 6.94% to 2.88%. A study by Lee et al. [18] uses an RSC controller paired with a voltage regulator to mitigate the harmonics. They improve the efficiency of the RSC controller by feeding the THD error due to each harmonic frequency instead of just the voltage error to the RSC.

A repetitive controller (RC) based active filter is shown in figure 2.3 [19]. A repetitive controller operation is based on the internal model principle (IMP). According to IMP, zero-error for any periodic signal can be tracked using a closed-loop as long as the reference generator is part of the loop. So theoretically, by using a repetitive controller, a high loop gain can be obtained at the Nyquist frequency, and any frequency below the Nyquist frequency can be removed.

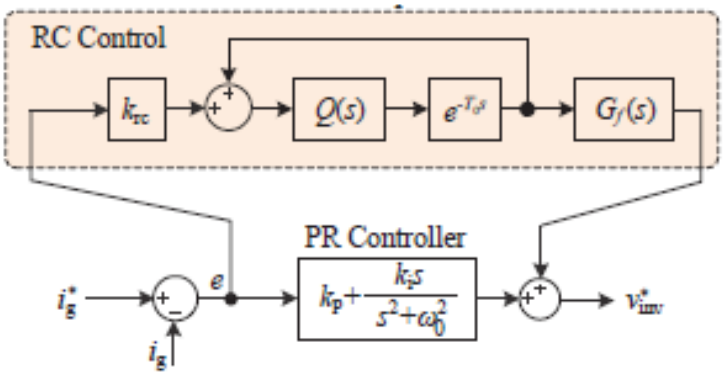

Figure 2.3. Repetitive controller connection

A study by Costa-Castello et al. [20] proposes an active filter based on RC. Their simulation and experimental results show that using an RC, high order harmonics can be removed and constant sinusoidal current output can be obtained. A study by Escobar

et al. [21] designs an active filter based on RC similar to the study mentioned above, but they alter the control loop of the RC to target only the odd-order harmonics. They achieve that by targeting and eliminating the negative sequence current injection. A study by Zhou et al. [22] combines an RC with an RSC to achieve selective harmonic elimination. They take advantage of the RC controller to obtain high loop gain which can be obtained using RC, and then uses multiple parallel RSC to identify and mitigate the harmonics that needs to be eliminated. Due to the pairing of RC with an RSC, the stability and the transient response of the system increases and becomes more cost-effective.

DB controllers can also be used for power quality improvement. They are based on designing complex algorithms to mitigate the harmonics. Unlike the methods mentioned above, DB designing is done in discrete time. They have a fast transient response, and selected harmonics can be targeted. They are not commonly used in power system applications as they are complex to design. Nowadays, there has been an increase in the use of multi-level converters. So, designing a DB controller for a multi-level controller is non-ideal and requires a lot of computing power which increases the overall cost of the system [23]. Also, as large of computation is required to meet the goals, it creates a time delay in the output, which also needs to be compensated.

Although the use of RC compared to DB for active filter design is more, RC has its own set of challenges. RC requires more memory to perform the tasks, which also creates a delay that needs to be compensated. Also, it has transient stability issues that need to be dealt with, which increases the overall cost of the system. Also, to remove selected harmonic frequencies, different loop gains need to be calculated and implemented, increasing the complexity of the system. Compared to RC and DB controllers, RSC are the easiest controllers to design and implement. The only challenge that presents itself during the use of RSC is frequency deviations due to high loop gains [24]. However, these issues can be dealt with pairing the RSC to a VCM, CCM or a HCM, as mentioned in 2.2.1.

2.3 Power quality improvement using battery

The use of ESS in microgrids has increased in the past decade to improve the RES fraction. RES fraction is the amount of energy from RES which can be supplied to the load. The energy that can be produced from RES is variable. For example, PV generation is only possible during day times and Wind energy generation is dependent on the wind speed, which may change during the course of the day. Let's suppose there is a microgrid with a PV plant. The demand for that microgrid reaches the peak at the evenings while during the daytime the demand is low. So, the power generated by PV although meets the demand and even exceeds it, but if there is no ESS integrated, the excess power gets wasted [25]. One way to cope with this problem is to feed the power from PV to the grid and supply the power to the load via grid i.e. Net metering. But this means that the power from spinning reserves would not alter that much and the advantage of integrating PV to reduce greenhouse gas emissions get eliminated. In this scenario, ESS integration is beneficial. It allows the storage of excess power and then uses it when the demand is high, lowering the overall energy supplied from the spinning reserves [26].

There are many studies available in the literature that present different algorithms and case studies to integrate ESS into the grid. Studies from Panayiotou et al. [27], Diaf et al., [28], Liu et al., [29] and Deotti et al., [30] are examples of different studies which investigate the feasibility and propose methods to integrate ESS into the microgrid. These studies generally just focus on maximizing the RES fraction and optimizing the cost of the RES. In this study, the focus is on the use of ESS for the power quality which is delivered to the grid and reduction of harmonics generated at the point of common coupling (PCC).

ESS systems can be used to store excess power and supply it for later use they can also help improve the power quality and mitigate harmonics. A study by Xu et al. [31] goes over the role of battery integration in removing unbalance in PCC in PV microgrids. In the literature, most of the work regarding power quality conditioning using batteries is related to wind farms. A study by Zeng et al. [32] discusses the benefits of

integrating the battery into wind farms to improve the power quality. Their results show that the battery absorbs the imbalance of power which is generated due to the variable nature of the wind. This absorption helps regulate the output power from the wind farms and keeps the voltage constant at the PCC. Similarly, a study by Mundackal et al. [33] also investigates the advantages of integrating the battery into wind farms. Their study focuses on showing how the battery can inject and absorb reactive power to the grid. This in turn helps in stabilizing the grid as well as improves the power flow to the load. Studies by Muyeen et al., [34] and Kirmani et al., [35] are examples of different works available in the literature which go over the power conditioning benefits of integrating the battery into wind farms. Studies by Guerrero et al. [36] and Ovaskainen et al. [37] goes over different control strategies for the IFC control for a battery integrated microgrid. However, their studies are limited distributed generators with constant power production, i.e., not RES.

2.4 Gaps in Literature

After extensive literature research regarding active filters and battery integration into the microgrid for power quality conditioning, the following gaps in the literature were found:

1) In the literature, there is research present regarding battery integration to increase the RES fraction and meeting demand. But there are few works available in literature that go over the power conditioning capabilities of the battery integration.
2) Even the works that go over the power conditioning benefits of integrating battery into microgrids do not present proper comparisons and detailed explanations.
3) No proper study is available which goes through the design process of IFC control for battery integrated microgrids.

Although it is not a research gap, one of the main reasons to conduct this study is that there is a 1 MW PV plant present in METU NCC. There are plans to integrate the

battery into the microgrid to increase the RES fraction. This study would help in the future for the IFC design.

CHAPTER 3

THEORY AND METHODOLOGY

3.1. Data

Solar irradiation and demand data that are used in this study are for our campus. They are collected from the sensors present in the solar farm. Hourly Data for irradiation and demand in a calendar year is used. For the simulations on MATLAB, one day was simulated at a time. For the simulation, 23rd June is selected for the irradiation data as it the longest day of the year and has the highest irradiance profile. So, the effect of battery integration on the harmonics can be adequately observed.

3.2. Model

The microgrid built in this study is shown in the figure 3.1. A 200 kW PV panel is connected to the grid via a 3-level neutral point clamped inverter (NPC). The voltage from the PV panel is controlled using a maximum powerpoint controller (MPPT). An incremental conductance method is used for the MPPT algorithm. A lithium-ion battery is also connected to the DC-link via a boost converter to control the charging and discharging of the battery. An RSC controller is paired with a voltage regulator for the IFC control. An LC filter is used as the passive filter to mitigate the high order harmonics. The power from the PV and the battery is fed to a 120 kV, 2500 MVA utility grid.

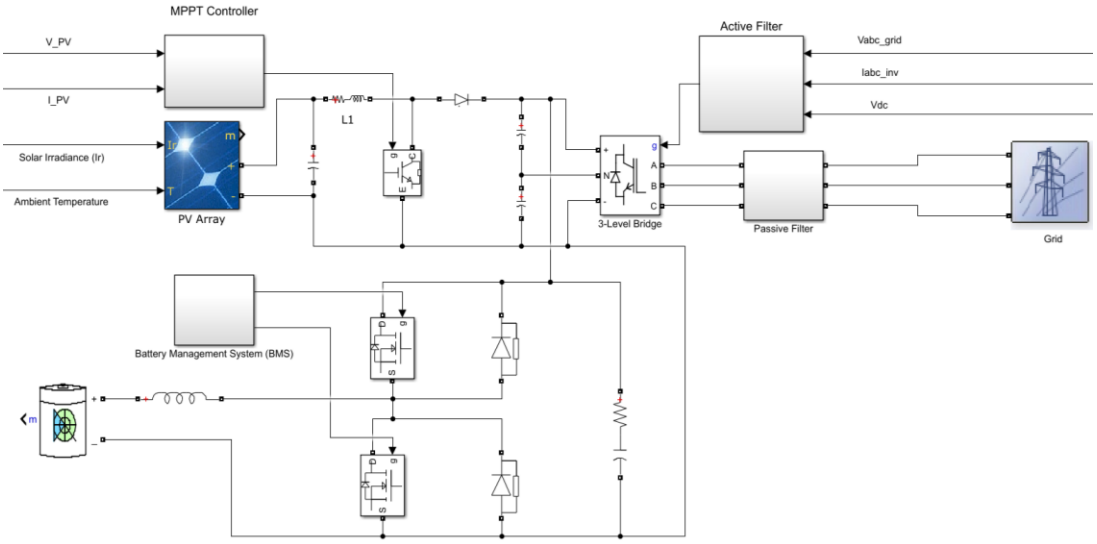

Figure 3.1. PV-Battery Microgrid

3.3. PV modeling

The beam radiation from the Sun incidences differently depending on the location on Earth. This is due to the Earth's rotation around the sun on its axis. That is why there are concepts on time zones. So, in order to have a proper comparison of optimal tilt angle between different locations the time has to be standardized. So, the first step is calculating the optimal tilt angle is to convert the standard time t_{std} to solar time t_s. Solar time represents the position of sun in the sky. In order to calculate the solar time, the longitude L_{loc} and time zone L_{std} of the location are taken into consideration along with the equation of time E. The equation of time is dependent on the day number n. Equations of time and solar time are found by equations 3.1, 3.2, and 3.3 [38].

$$B = \frac{(n-1)360}{365} \tag{3.1}$$

$$E = 229.2(0.0000075 + 0.001868\cos(B) - 0.032077\sin(B) - 0.014615\cos(2B) - 0.04089\sin(2B)) \tag{3.2}$$

$$t_s = t_{std} + \frac{4(L_{std} - L_{loc}) + E}{60} \tag{3.3}$$

Solar time gives us a relation between any position on Earth and the position of the sun. This helps in standardizing the tilt angle calculated between different locations. In order to use the solar time in our calculations, it is converted to angle called hour

angle ω by taking into account that Earth rotates 15° per hour. It is negative for mornings and positive for afternoon. It can be calculated by equation 3.4 [38].

$$\omega = (t_s - 12) \times 15 \tag{3.4}$$

Another parameter which changes depending on the location is the Latitude φ. Latitude represents the angular position of a location North or South with respect to the equator. The rotation of the Earth around the sun is on a fixed axis but the axis also has a slight tilt due to which the angular position of the sun does not remain constant. So, it also has to be taken into account when calculating the tilt angle. Declination Angle δ is used for this purpose. It represents the angular position of Sun at noon with respect to the equator. It is calculated by equation 3.5 [38].

$$\delta = 23.45 \sin\left(360\left(\frac{284 + n}{365}\right)\right) \tag{3.5}$$

Another parameter related to the location which is taken into consideration is the surface azimuth angle γ. It is defined as the angle between the South and projection on a horizontal of the normal to the surface. Its value is between -180° and +180°. It is taken as negative for East of South and positive for West of South.

Now the tilt angles can be calculated using the parameters above. First, the zenith angle θ_z and the solar altitude angle α_s are calculated. Zenith angle is the angle between vertical (normal to the horizontal) and beam radiation. It can calculated from equation 3.6 [38].

$$\cos(\theta_z) = \cos(\phi)\cos(\delta)\cos(\omega) + \sin(\phi)\sin(\delta) \tag{3.6}$$

Solar altitude angle is just the complement of the Zenith angle. The solar azimuth angle γ_s is the angle between South and the projection of beam radiation on horizontal surface. It is dependent on the sign of the hour angle, zenith angle, latitude and the declination angle. It can calculated from equation 3.7, 3.8 and 3.9 [38].

$$sign(\omega) = \begin{cases} -1, & \omega < 0 \\ 1, & \omega \geq 0 \end{cases} \tag{3.7}$$

$$\gamma_s' = \begin{cases} \dfrac{\cos(\theta_z)\sin(\phi) - \sin(\delta)}{\sin(\theta_z)\cos(\phi)}, & \theta_z \neq 0 \\ 1, & \theta_z = 0 \end{cases} \tag{3.8}$$

$$\gamma_s = \begin{cases} sign(\omega)|\cos^{-1}(\gamma_s')|, & \gamma_s' \neq 1 \\ 0, & \gamma_s' = 1 \end{cases} \quad (3.9)$$

Now the angle of incidence θ can be calculated. It is done for three different tracking schemes. First is without any tracking. It is the angle between the beam radiation on a surface and the surface normal. It can be calculated using equation 3.10 [38].

$$\cos(\theta) = \cos(\theta_z)\cos(\beta) + \sin(\theta_z)\sin(\beta)\cos(\gamma_s - \gamma) \quad (3.10)$$

For single axis E-W tracking, the angle of incidence can be calculated using equation 3.11 [38].

$$\cos(\theta) = [1 - \cos^2(\delta)\ \sin^2(\omega)]^{1/2} \quad (3.11)$$

For 2-axis tracking, the angle of incidence will be same always as the panels will be adjusted in real time such that the beam radiation always incidence perpendicular to the surface [4].

Using the solar geometric relations and irradiation data the energy generation can be calculated. First, we need the extraterrestrial normal insolation $I_{o,n}$. It is the normal solar radiation unaffected by the Earth's atmosphere. It can be calculated using equation 3.12 [38] where G_{sc} is the Solar constant equal to 1367 W/m$^{2.}$

$$I_{o,n} = G_{sc}(1 + 0.033\cos(\frac{360}{365}n)) \quad (3.12)$$

From the extraterrestrial normal irradiation the extraterrestrial irradiation I_o is obtained using equation 3.13 [38].

$$I_o = I_{o,n}\cos(\theta_z) \quad (3.13)$$

From the Extraterrestrial irradiation and the DNI data given in the TMY dataset, the clearance index k_T can be calculated. It gives us the frequency distribution of cloud cover. It is always between 0 and 1. The clearance index can be calculated by equation 3.14 [38].

$$k_T = \frac{I}{I_o} \quad (3.14)$$

From the clearance index, the horizontal diffuse irradiation I_d can be found. The relation between it and clearance index is given by Orgil and Holland's correlation. It is given in equation 3.15 [38].

$$\frac{I_d}{I} = \begin{cases} 1 - 0.294k_T & k_T < 0.35 \\ 1.577 - 1.84k_T & 0.35 < k_T < 0.75 \\ 0.177 & k_T > 0.75 \end{cases} \quad (3.15)$$

Once the diffuse irradiation is obtained, the beam irradiation I_b can be obtained. The horizontal global irradiation consists of beam, diffuse and reflected irradiation. In this research, the reflected irradiation is neglected. The beam irradiation is calculated with equation 3.16 [38].

$$I_b = I - I_d \quad (3.16)$$

From this beam irradiation, the normal component of beam irradiation $I_{b,n}$ which incidences on the surface can be calculated. It is given by equation 3.17 [38].

$$I_{b,n} = \frac{I_b}{\cos(\theta_z)} \quad (3.17)$$

Now as the PV modules are tilted to some angle in order to maximize the power generation, the beam radiation $I_{b,T}$ and diffuse irradiation $I_{d,T}$ component changes. It can be accounted for using equations 3.18 and 3.19 [38].

$$I_{b,T} = I_{b,n}\cos(\theta) \quad (3.18)$$

$$I_{d,T} = \frac{I_d(\cos(\beta) + 1)}{2} \quad (3.19)$$

The energy production from PV modules is not only dependent on solar irradiation but also the type of PV module used. Many factors affect the energy production such as the ambient temperature, T_{amb}, the normal operating cell temperature, *NOCT*, which is the cell temperature when a PV cell is tested at the NOCT irradiance, $G_{ref,\,NOCT}$, at an ambient temperature, $T_{ref,\,NOCT,}$ and wind speed of 1 m/s under no load. The temperature coefficient, β_{ref}, shows how the maximum power and efficiency, η_{PV}, changes as the cell temperature changes by 1°C. These are reported at standard test conditions of cell temperature, T_{STC}, and irradiance, G_{STC}. The efficiency at STC is $\eta_{PV,\,ref}$. For this research, the PV module Axitech 250W is considered. Its specifications are obtained from its datasheet. These specifications are shown in table 3.1 [39].

Table 3.1. Specifications of Axitech 250 W PV Panel

$\eta_{PV,ref}$	0.1537
Area (m^2)	1.63
Peak Power (W)	250
G_{STC} **(W/m^2)**	1000
T_{STC} **(°C)**	25
NOCT (°C)	45
$G_{ref,\ NOCT}$ **(W/m^2)**	800
$T_{ref,\ NOCT}$ **(°C)**	20
β_{ref} **(1/K)**	0.0042

As mentioned above, the efficiency given on the datasheet is for standard test conditions. When solar irradiance incidences on the PV module, the cell temperature goes up which in turn changes the efficiency of the module. This change in cell temperature change can be calculated by equation 3.20 [38].

$$T_{cell} = T_{amb} + \frac{(NOCT - T_{ref,NOCT})I}{G_{ref}} \tag{3.20}$$

Once the cell temperature is calculated, new efficiency under this temperature can be calculated. It is given by equation 3.21 [38].

$$\eta_{PV} = \eta_{PV,ref}(1 - \beta_{ref}(T_{cell} - T_{STC})) \tag{3.21}$$

The power generated by single module can be calculated by equation 3.22 [38].

$$I_{PV} = \eta_{PV} I_T \tag{3.22}$$

Finally, the energy production for the whole plant can be calculated by equation 3.23 [38].

$$E_{gen} = I_{PV} \times Area \times Number\ of\ Modules \tag{3.23}$$

3.3. PV control modeling

The power supplied by the PV panels is variable. It depends on the irradiation falling on the panels as discussed above so we need to make sure power supplied is regulated and maximum power is generated. To achieve this goal, a boost converter is used. In the boost converter, the pulses for the switch should be supplied such that the maximum power is obtained at the output.

The pulses for the switch are obtained through the Incremental Conductance method (ICM). ICM uses a simple mathematic principle that the value of a variable at which a function is maximum can be calculated by finding the value of the variable at which the first derivative of the function is zero.

The derivative of power with respect to the voltage is given by equation (3.24).

$$\frac{dP}{dV} = \frac{d(V.I)}{dV} = I\frac{dV}{dV} + V\frac{dI}{dV} = I + V\frac{dI}{dV} \tag{3.24}$$

So in order to attain Maximum Powerpoint (MPP),

$$\frac{dI}{dV} = -\frac{I}{V} \tag{3.25}$$

So the value $-\frac{I}{V}$ is calculated and compared with the reference which is zero and the error is sent to a built in DC/DC converter PWM generator block to obtain the gating signals for the boost converter switch. The MPPT controller designed in MATLAB is shown in figure 3.2.

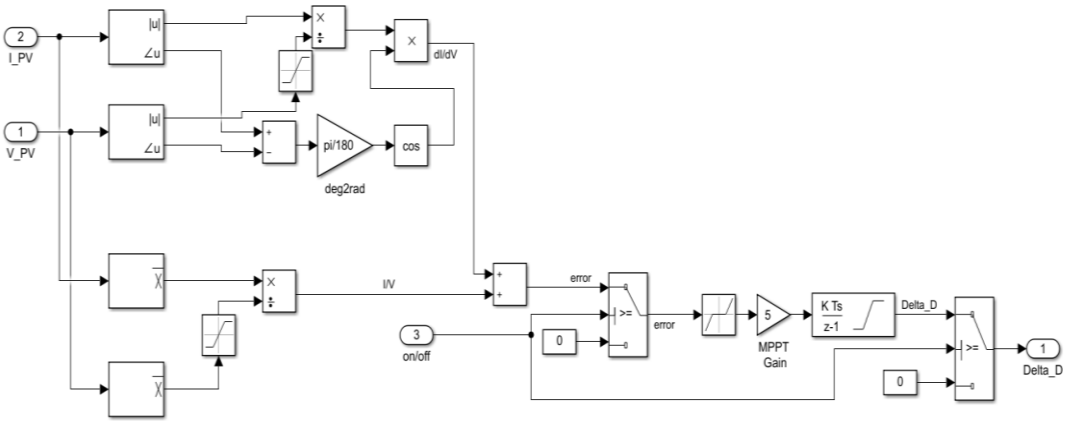

Figure 3.2. MPPT controller

3.4. Interfacing Converter

A multi-level converter is used as the IFC for this study. They have higher efficiency and a better harmonic profile. The interfacing converter used in this study is a 3-level Neutral Point Clamped inverter. IGBT's are used as switching elements. It is shown in the figure 3.2. It is a bidirectional converter which means that the power can flow in both directions.

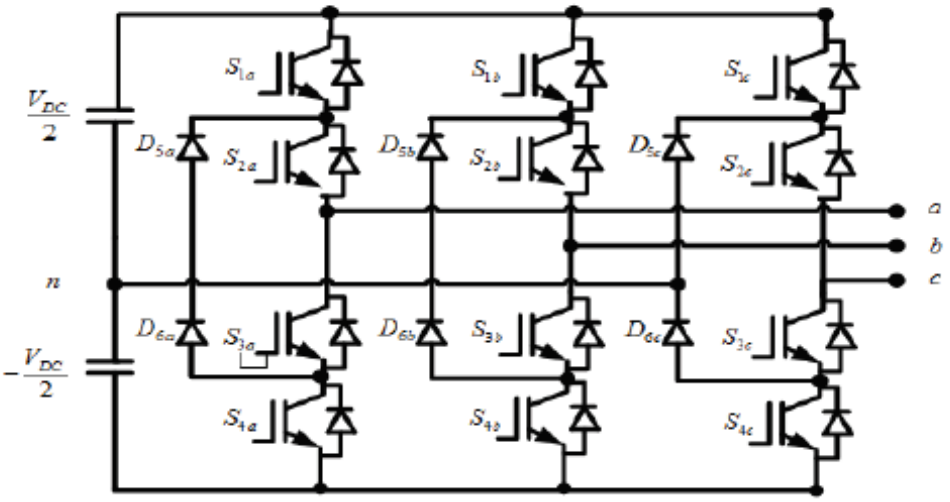

Figure 3.3. 3-phase 3-level NPC

There are four switches for each phase in this converter. S_{1a}-S_{3a} and S_{2a}-S_{4a} are complementary, meaning they cannot be open or closed at the same time. Based on

the switches, 3 possible voltage levels can be obtained at the output. The switching scheme is shown in the table below.

Table 3.2. Switching schemes of 3-phase 3-level NPC

S_{1a}	S_{2a}	S_{3a}	S_{4a}	V_{an}
1	1	0	0	$+0.5V_{DC}$
0	1	1	0	0
0	0	1	1	$-0.5V_{DC}$

According to Fourier Transform, any waveform can be expressed as:

$$V_o = a_0 + \sum_{n=1}^{\infty} a_n cos(n\theta) + b_n sin(n\theta) \tag{3.26}$$

Now, as the voltage output from a 3 phase 3-level inverter has odd quarter-wave symmetry:

$$a_0 = 0 \tag{3.27}$$

$$a_n = 0, for\ all\ n \tag{3.28}$$

$$b_n = 0, for\ even\ n \tag{3.29}$$

So,

$$V_o = \sum_{n=1}^{\infty} b_n sin(n\theta) \quad , for\ n = 1,5,7,11\ldots \tag{3.30}$$

Where,

$$b_n = \frac{4V_{dc}}{n\pi} \sum_{k=1,5,7\ldots}^{n} (-1)^{k+1} cos(n\alpha_k) \tag{3.31}$$

The advantage of using a 3 phase 3-level inverter is that, even and triplen frequencies are zero so only 5^{th} and 7^{th} order harmonics are the harmonics which are considered to improve the power quality. As discussed in the literature, the higher-order harmonics can be removed using a passive filter at the output.

3.5. IFC Control

In the literature research, different methods for the IFC control for harmonics mitigation are mentioned. In this research, a Voltage Controller is used with a RSC to filter out the harmonics while accounting for the voltage unbalance. The IFC control system is shown in figure 3.3. Voltage from the grid, DC voltage from the DC link capacitor and output current from the inverter are the input of the IFC control. First, the fundamental frequency is obtained using a phase locked loop (PLL). The fundamental frequency is essential to obtain as it is used in frame of reference conversion which is done multiple times in the control loop. The current command which will be used for the RSC is obtained in the current command generator. The current command obtained is compared with the instantaneous current output from the converter and the error is fed to the RSC. The instantaneous current is also sent to the impedance compensator. The total voltage command from the RSC and the impedance compensator are summed up and sent to the voltage command generator. From the figure 3.3 it can be seen that, the voltage command is time invariant frame of reference (dq), so it needs to be converted to time variant frame of reference (abc). This is done in the voltage command generator. A simple dq to abc converter block cannot be used as timing delays due to sampling, computation and the leakage inductance needs to be addressed. Once the reference voltage is obtained, it is sent to the PWM generator, where is it compared with two level shifted triangular carriers to generate PWM signals for the IFC.

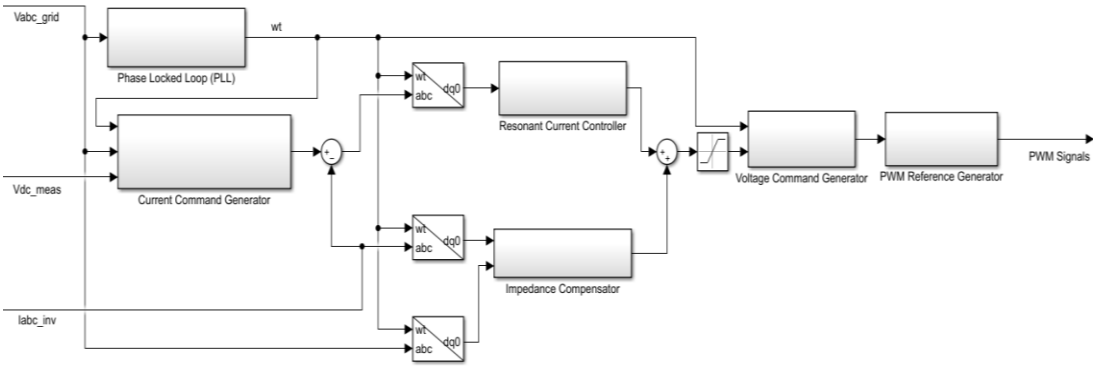

Figure 3.4. IFC control

3.5.1. Current Command Generator

The Current Command Generator is shown in the figure 3.4. It has two constituent blocks, reference current command generator and harmonic current command generator. The reference current command generator is used to maintain the DC-link voltage and regulate the reactive power transfer. The harmonic current command generator is used to generate the commands for the 5^{th} and 7^{th} harmonic mitigation which will be used in RSC block.

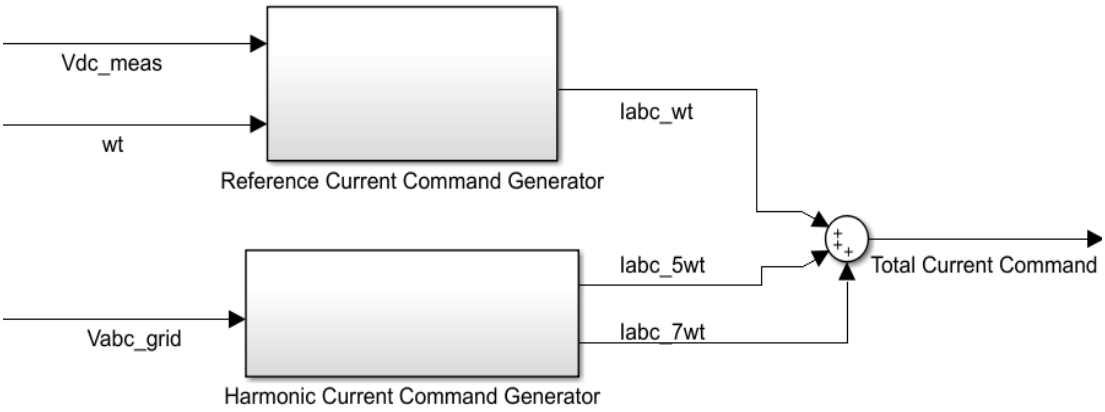

Figure 3.5. Current command generator

The Reference Current Command Generator is shown in figure 3.4. The instantaneous voltage at the DC link capacitor is compared with the reference voltage which is set at '500 V'. A PI controller is used to smoothen the error signal. The error is fed into a dq to abc frame converter to obtain reference current command in time varying frame of reference. The angular frequency is obtained through a PLL block as mentioned

previously. ‘d’ is kept zero while the error is sent to ‘q’ because the IFC control is based on the assumption that the power converter is ideal and the active power at the input and output of the converter is same. So, by setting the error to ‘q’, the reactive power can be regulated and compensated.

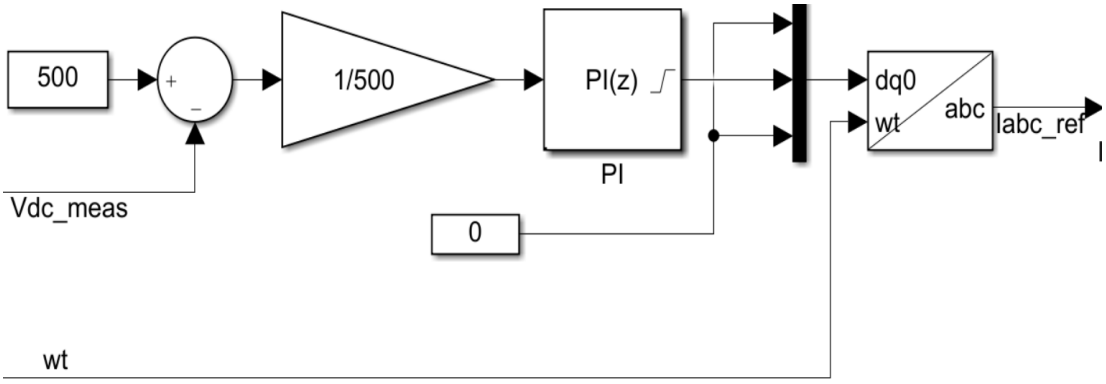

Figure 3.6. Reference current command generator

The harmonic current command generator is shown in the figure 3.6. This block is used to obtain the 5th and 7th harmonic reference. The harmonic current command is calculated by the equation 3.31.

$$I_{h\prime abc} = V_{h\prime abc} \times G_h \tag{3.32}$$

$V_{h'abc}$ is the harmonic component and the G_h is the conductance command. The harmonic command can be obtained at conversion from the signal from the time variant frame of reference to time invariant frame of reference with the input frequency being the harmonic frequency and then back to time variant frame of reference. The harmonic frequencies are obtained in a different block by multiplying the fundamental frequency from the PLL to the harmonic order. The conductance command is obtained from the Tuning Controller which is shown in the figure 3.7. The tuning controller block is used to calculate G_h. G_h is basically the error between the THD from a certain harmonic component and the reference THD. The reference THD is set as “2%”. The THD is calculated according to the equation 3.32. A high pass and a lower pass filter is used to smoothen to the signals during the calculation of THD.

$$THD_h = \frac{V_{h,rms}}{V_{rms}} \tag{3.33}$$

After obtaining the reference current command and the harmonic current command, they are summed up to obtain the total current command which is sent to the next block.

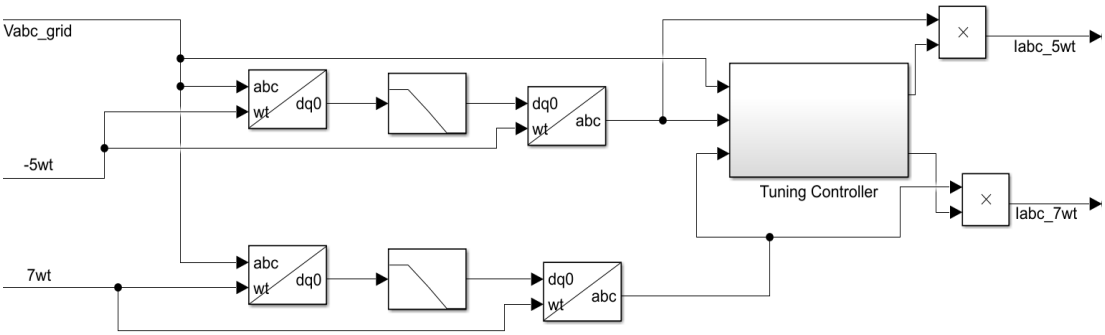

Figure 3.7. Harmonic current command generator

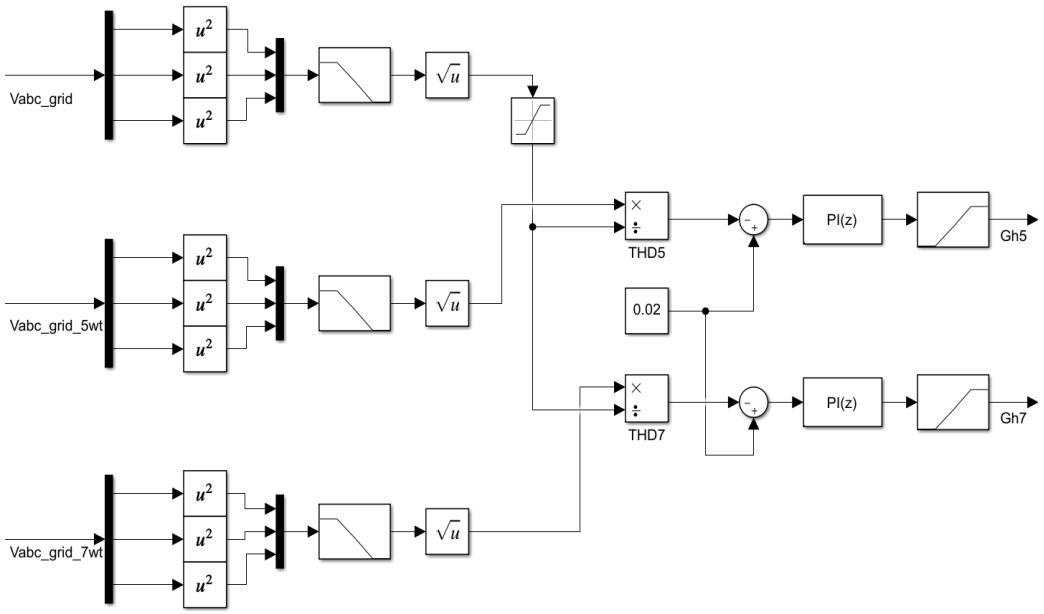

Figure 3.8. Tuning controller

3.5.2 Resonant Current Regulator (PR controller)

RSC are one of the best controllers to use to mitigate the harmonics as mentioned in the literature review. In theory, at the resonant frequency the RSC has infinite gain. So, by connecting parallel RSC at certain harmonics, that harmonic content can be removed. In this research, we focus on the 5th and the 7th harmonic as they have the biggest impact on the output signal and higher frequencies can be easily removed through a passive filter at the inverter output as mentioned in the literature review. The transfer function of a RSC is given by equation 3.33.

$$G_h(s) = K_p + \sum_{h=5,7} \frac{K_i \times 2\omega_h \xi \times s}{s^2 + 2\omega_h \xi s + {\omega_h}^2} \tag{3.34}$$

Where K_p is the proportional gain, K_i is the integral gain, ξ is the damping factor and ω_h is the harmonic frequency. However, this equation is for continuous time but our model is created for the discrete time so we need to convert it into discrete time. Conversion is done through MATLAB's "c2d" function. The general form of the PR controller equation in discrete time is given in equation 3.34. The PR controller is shown in the figure 3.9.

$$G_h(z) = K_p + \sum_{h=5,7} \frac{A_h z + B_h}{z^2 + C_h z + D_h} \tag{3.35}$$

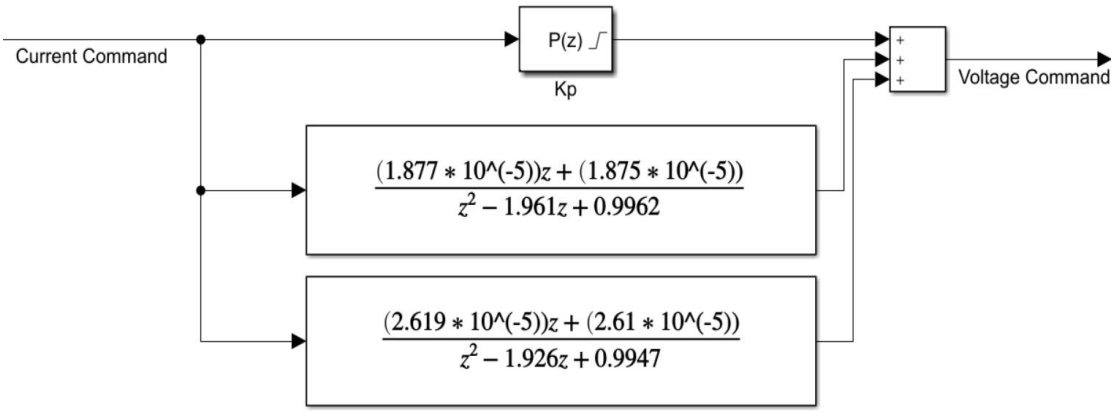

Figure 3.9. RSC controller

3.5.3 Impedance Compensator

In the IFC control, one of the inputs is Voltage after the transformer (V_{grid}). Due to transformer, there will be a loss due to leakage and choke impedance. So these impedances needs to be compensated to ensure proper PWM signal generation. This is done in the impedance compensator block. It is shown in the figure 3.10.

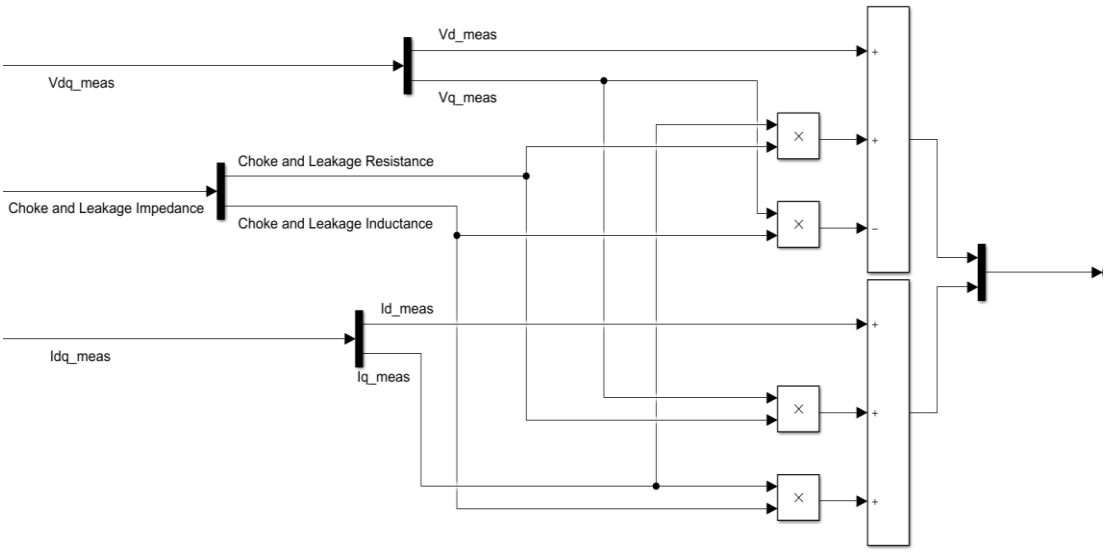

Figure 3.10. Impedance compensator

3.5.4 Reference Voltage Generator

The voltage obtained from the RSC and the impedance compensator are in time invariant frame of reference. So, it needs to be converter to time variant frame of reference. But a simple ‘dq’ to ‘abc’ converter cannot be used for this transformation. Due to computation, there is a timing delay which needs to be accounted for. Similarly, due to the choke impedance, phase shift can also be produced which needs to be accounted for. This is done in the reference voltage generator block as shown in figure 3.11.

3.6. Battery Management System (BMS)

Battery used in this study is a Lithium-Ion (Li-ion) battery. It is interfaced to the main microgrid via boost converter to control the charging and discharging of the battery. The gating signals of the boost converter are controlled using a BMS system. The BMS algorithm is shown in the figure 3.12. The battery is charged only when there is excess amount of PV generated.

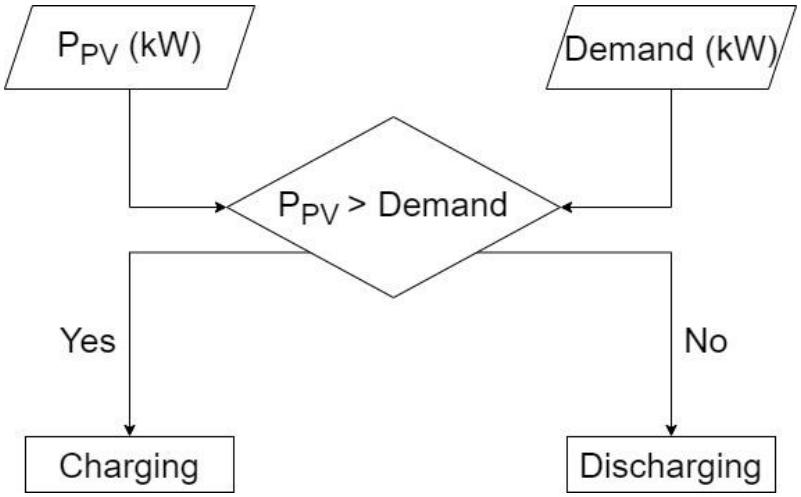

Figure 3.11. BMS algorithm

3.7. Battery use for harmonic mitigation

A study by Yang et.al., [19] shows the relation between DC-link voltage and the deadtime during IFC switch's off and on time. They mention that by stabilizing the DC-link voltage, the harmonics caused due to the deadtime. Equation 3.36 shows the maximum deadtime t_d where f_{sw} is the switching frequency, V_{grid} is the grid voltage, I_{grid} is the grid current, ω_0 is the fundamental angular frequency and L is inductance of the passive filter at the output.

$$t_d = \frac{1}{2f_{sw}}\left(1 - \frac{V_{grid} + \omega_0 L I_{grid}}{V_{DC}}\right) \tag{3.36}$$

A study by Lu et.al., [40] relates the reactive power developed at the output of the converter with the DC-link voltage at the input. They mention that stability of the grid

gets compromised if there is not proper control of reactive power present. Especially in case of weak grid, the injection of reactive power can cause the malfunction of the grid.

After observing the microgrid after integration of battery in figure 3.1, the voltage at the inverter V_{inv} during charging and discharging is written in equation 3.35 and 3.36 respectively. V_{PV} is the voltage from the PV system and $V_{Battery}$ is the voltage from the battery.

$$V_{inv} = V_{PV} - V_{Battery} \quad \text{(charging)} \tag{3.37}$$

$$V_{inv} = V_{PV} + V_{Battery} \quad \text{(discharging)} \tag{3.38}$$

So from equation 3.35 and 3.36, it can be seen that by integrating a battery into the microgrid will help stabilize the DC-link voltage. During periods when the power from PV grid is less or more, the battery would stabilize the voltage at the DC-link accordingly through charging and discharging. This DC-link stabilization would in turn help the IFC control to function more efficiently in mitigating the harmonics. Batteries are also useful in injecting and absorbing reactive power which help the IFC for reactive power compensation. In turn the overall reactive power developed at the output decreases.

CHAPTER 4

RESULS AND DISCUSSION

Using the irradiance data and the theory mentioned in section 3.3, PV is modelled on 'excel' to obtain the optimal tilt angle for maximum power generation. In this study, a 200 kW PV system is modelled. The optimal tilt angle for our campus is calculated as 33º. Using the tilt angle the beam irradiation on the PV panels can be calculated, using which we can obtain the total power generated. As mentioned in section 3.1, the PV system is modelled according to the irradiation data of METU NCC. The proposed system simulates a complete day. The day selected for this study is 23rd June as it is one of the longest days in the year and healthy amount of solar power is produced so the validity of the proposed system can be confirmed. The power generation estimated for our PV system for 23rd June is shown in figure 4.1.

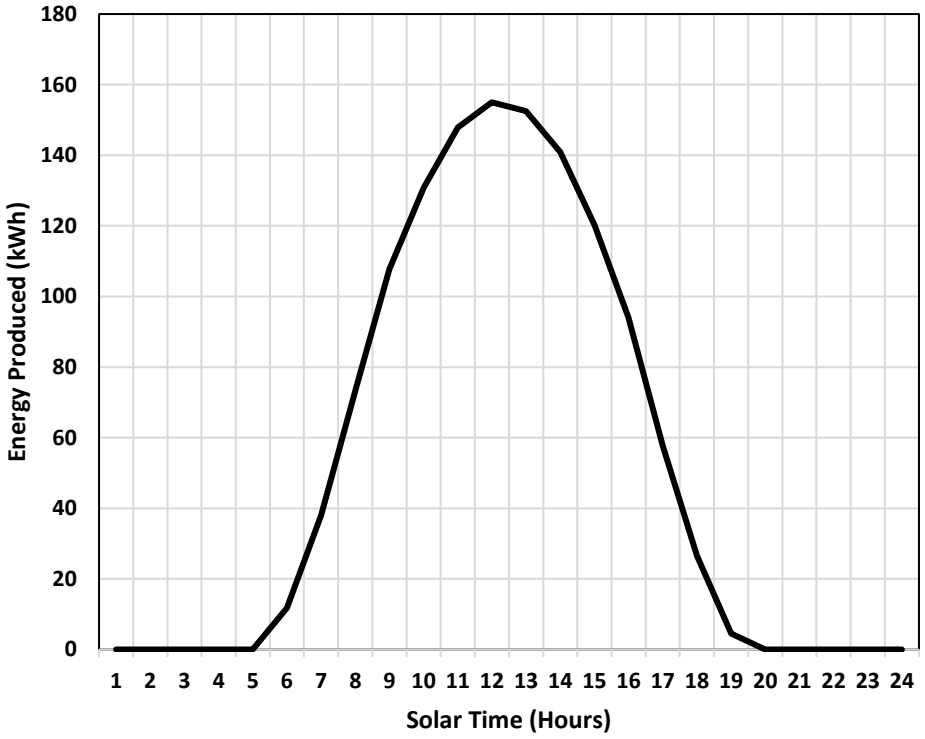

Figure 4.1. Theoretically calculated energy generation on 23rd June

Before discussing the THD and the benefits of integrating battery into the microgrid, the validity of our system needs to be confirmed. After running the simulation, the power generated from our PV system can be obtained. The PV power generated, and the demand is shown in the figure 4.2. From the figure 4.2, it can be observed that the maximum power obtained through simulation and theoretically is around 160 kW. This means that our system is working and is valid.

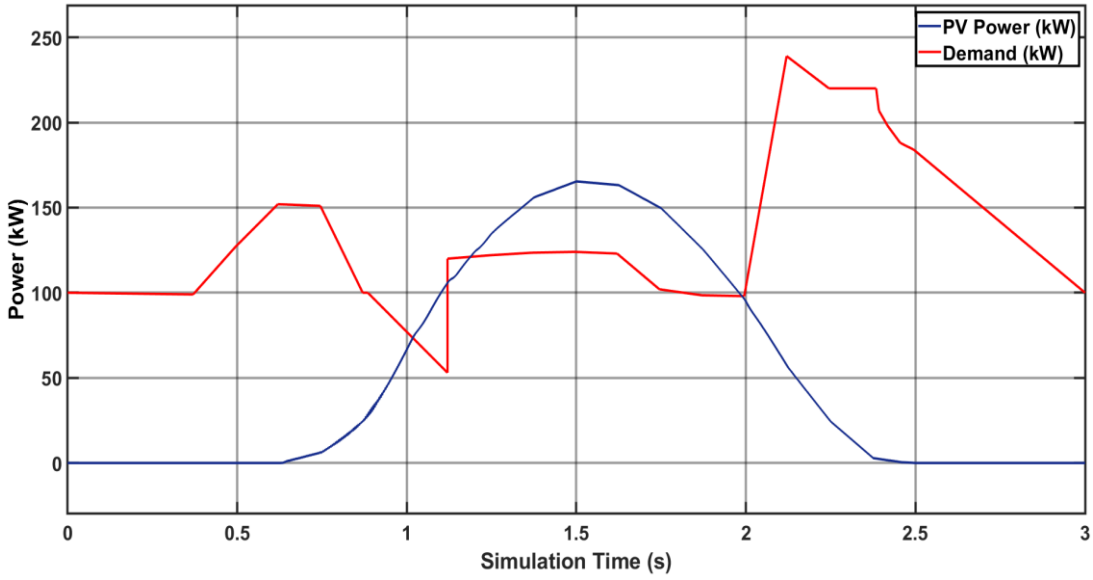

Figure 4.2 Simulated PV power generation and demand data for 23rd June

The DC-link voltage (V_{DC}), state of charge (SOC) and power generated from PV system (P_{PV}) is shown in figure 4.3. Whenever, P_{PV} exceeds the demand, the battery starts charging and storing the excess power. And as soon as the P_{PV} is less than the demand, the battery starts discharging and supplies power to the load. The switching time of the battery can be seen in appendix A. Hence, the SOC increases from the period from '1 sec' to '2 sec'. It can also be observed that during the switching of battery state from charging and discharging, there is a voltage unbalance in the DC-link voltage. This unbalance is due to the change in the current direction in the DC-link. But this unbalance is easily compensated through the IFC control and the V_{DC} is kept constant at '500 V' which is the reference voltage set in the IFC control.

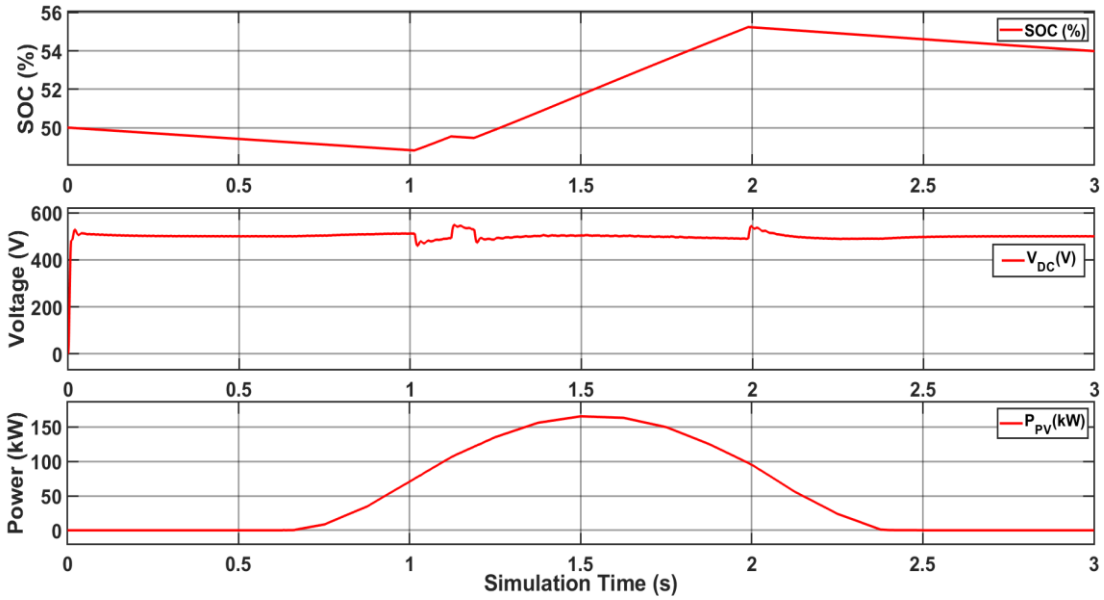

Figure 4.3. SOC, DC-link Voltage and PV power generation

For this research, the microgrid is simulated for two cases. Once it is run without battery integration and once with battery integration. Then the voltages and the THD are obtained and compared for both cases to observe the benefits of integrating battery into the microgrid. The parameters for the controllers are modelled through the PID tuner available in MATLAB. The parameters of the controller for both PV-battery and PV microgrid are shown in table 4.1. The parameters are generally same both cases but for the reference current controller, the parameters change. This is expected as the DC-link voltage profile is different for those two cases.

Table 4.1. Controller parameters

Controller	Parameter for PV microgrid	Parameter PV-Battery microgrid
Reference current controller	k_p=1 k_i=700	k_p=6 k_i=100
Tuning controller	k_p=1 k_i=500	k_p=1 k_i=500
Resonant current controller	k_p=0.3 k_i=100	k_p=0.3 k_i=100

A 3-level NPC converter is used as the IFC converter as mentioned in section 3.4. It used to converter the DC power coming from the PV and battery to AC and send it to the grid. The IFC's gating signals are generated using the control system described in

section 3.5. Figure 4.4 shows the unfiltered IFC output voltage for PV-battery microgrid. Hence, it is squarer shaped and has sharp peaks. As mentioned above, due to switching of charging states of the battery, there are some voltage unbalances in the DC-link voltage which also cause the voltage unbalance at the converter output. Figure 4.5 shows the filtered IFC output voltage for PV-battery microgrid. This voltage is obtained after the voltage passes through the passive filter. The passive filter removes the high order harmonics; hence the voltage looks more sinusoidal and is smoother. To compare the two cases, the unfiltered and filtered IFC output voltage for both cases is shown in the figure 4.6 and 4.7, respectively. After comparing the voltages from both cases, it is obvious that the voltage obtained from PV microgrid is smoother when compared to PV-battery microgrid. But the voltage output for PV microgrid shows a slight variation during the course of simulation. Whereas the voltage output for the PV-battery microgrid is generally constant at a certain magnitude whether it is filtered or not. Although there are slight unbalance due to changing of switching states, the voltage is constant for PV-battery microgrid.

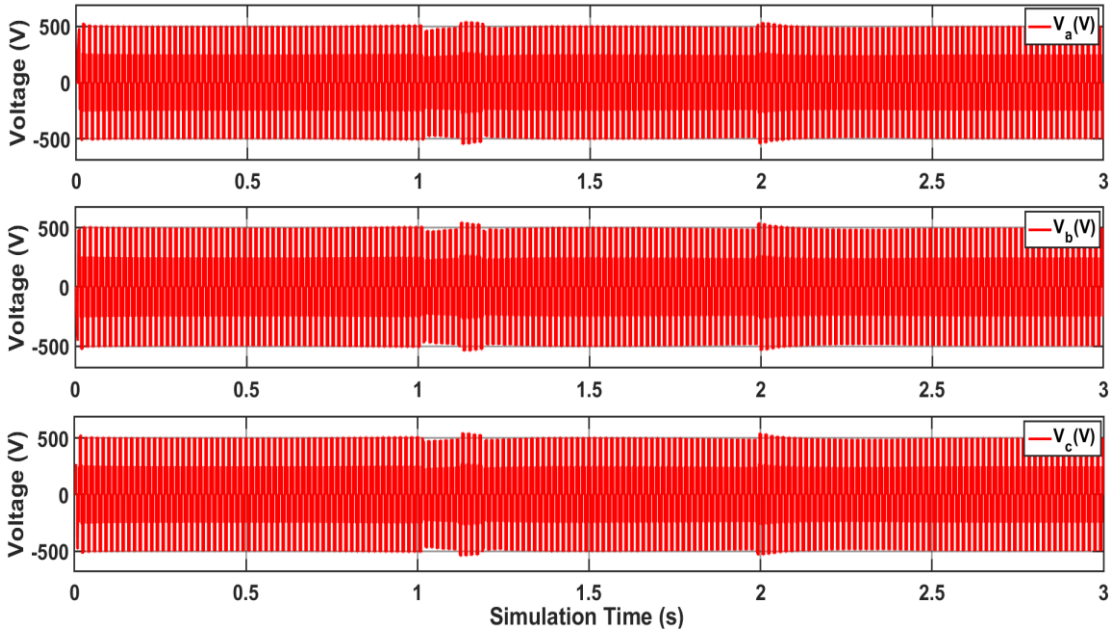

Figure 4.4. Unfiltered IFC output voltage for PV-battery microgrid

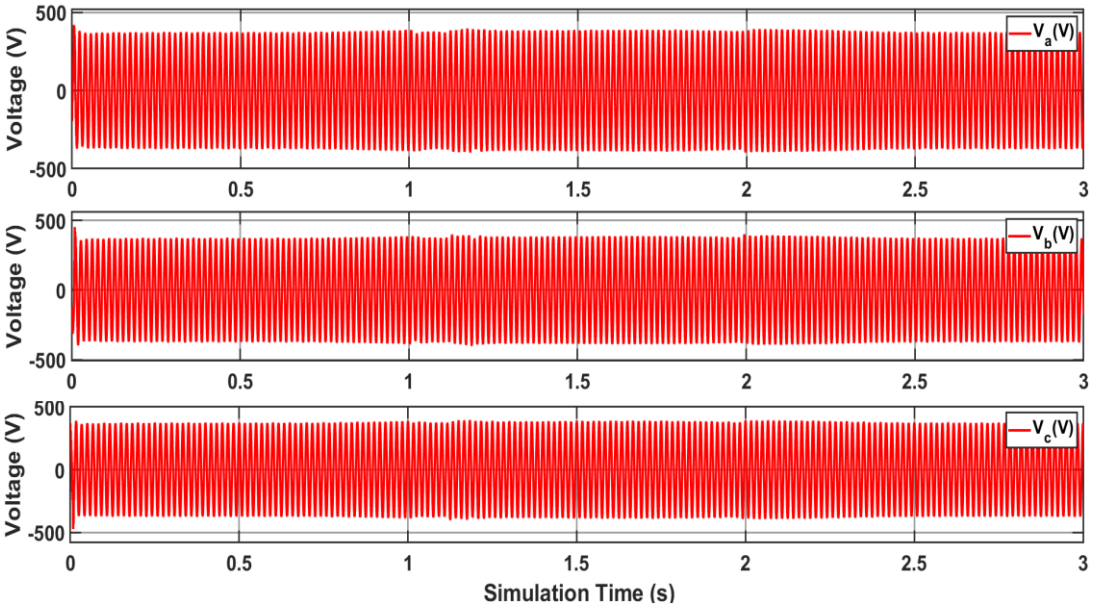

Figure 4.5. Filtered IFC output voltage for PV-battery microgrid

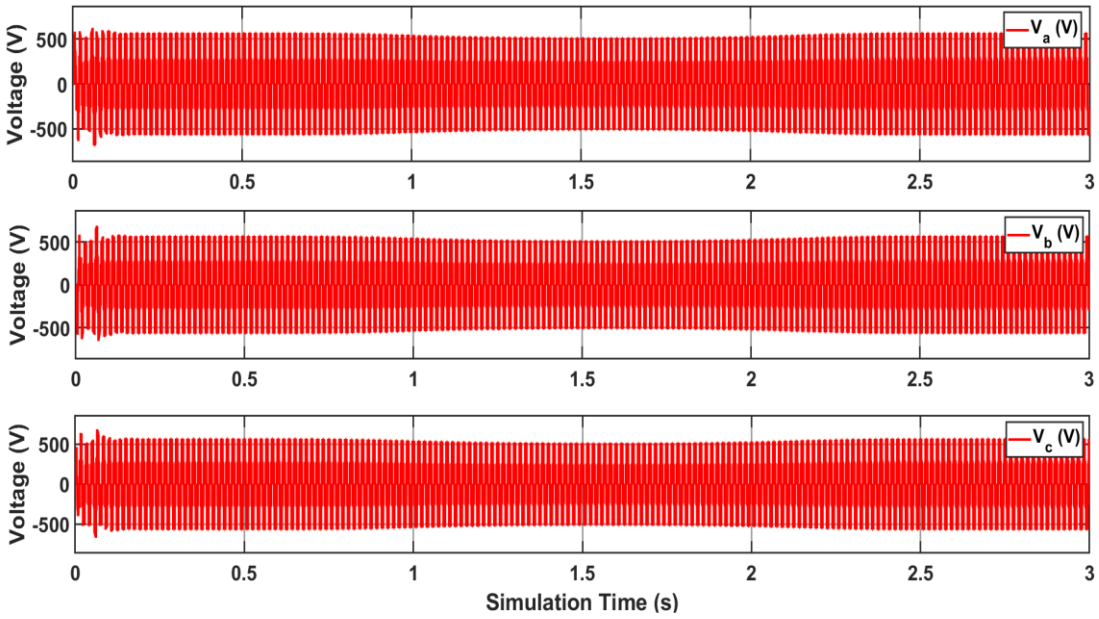

Figure 4.6. Unfiltered IFC output voltage for PV microgrid

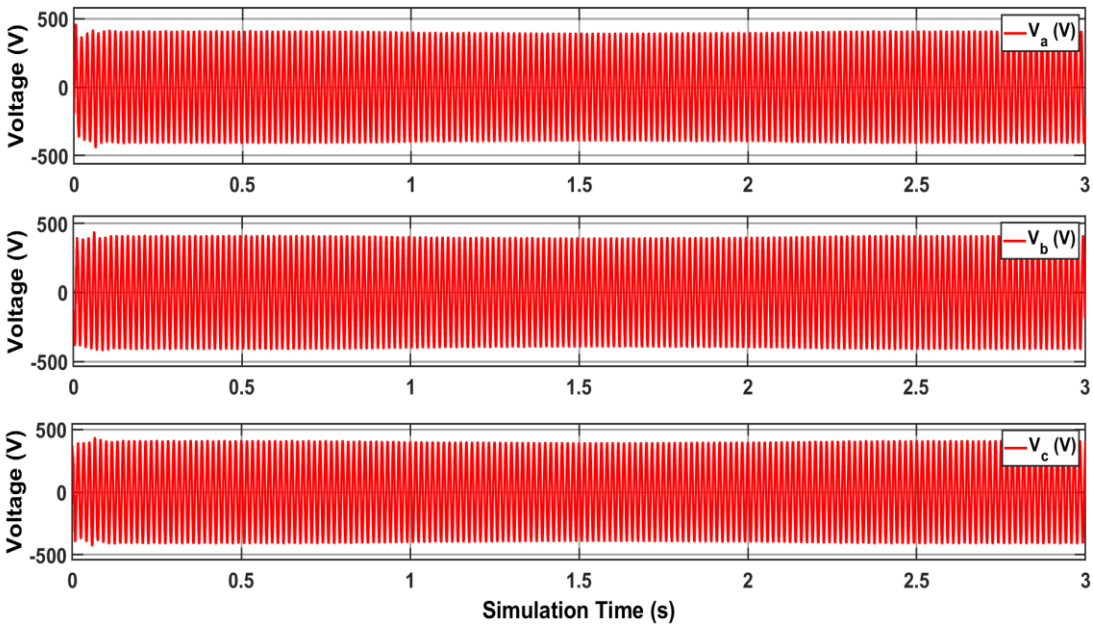

Figure 4.7. Output voltage from the converter after filtration for PV microgrid

To verify the effect of battery integration into the microgrid on the harmonics of the voltage output, the THD comparison needs to be done. THD for both cases is obtained through Fourier transform. Figure 4.8 and 4.9 shows the THD graph for unfiltered voltage output for PV and PV-battery microgrid respectively. Figure 4.10 and 4.11 shows the THD graph for filtered output voltage for PV and PV-battery microgrid respectively. The THD for unfiltered output voltage without battery integration is 33.89% and after filtration it reduces to 2.34%. Whereas after battery integration the THD for unfiltered voltage is 40.45% and after filtration it is 1.89%. Also, it can be seen that after filtration the magnitude of the voltage at the fundamental frequency also reduces. It is understandable as there is reduction of harmonics and loss in voltage after going through the passive filter. The THD values for individual harmonics can be seen in appendix B.

After comparing the THD values for both cases, it can be observed that integration of battery into the microgrid increases the THD of unfiltered voltage. This is due to an additional current path and switching of current direction during change in charging states of the battery. But if the THD after filtration, the THD for PV-battery microgrid is lower than the THD for just PV microgrid. This shows that integration battery

increases the higher order harmonics, but it complements the IFC control in reducing the lower order harmonics. Higher order harmonics are removed using the passive filter for those cases. As the IFC control is not responsible for controlling the higher order harmonics, due to the additional current path they increase whereas the lower order harmonics reduce. This can be explained through the theory described in section 3.7. Due to integration of battery, the DC-link voltage becomes more stable. In reference current command generator, the DC-link voltage is compared with the reference DC-link voltage and as the after integrating the battery, the DC-link voltage is more stable, the IFC control works with a higher efficiency as the error due to voltage variation is less and the current command signal mostly contains the information about the harmonics which are then mitigated. Figure 4.12 shows the DC-voltage error signal for both cases. It can be seen that the DC-link voltage after battery integration is easily kept constant and slight amount of error is present whereas the error without battery integration is constantly changing. The change is due to the fact that the power delivered through the PV panels is changing during the course of the simulation and there is no battery present to regulate the voltage. The only issue with integrating a battery into the microgrid, is the voltage unbalance causes during the switching of charging states. But this voltage unbalance can also be mitigated using a more sophisticated BMS. A better BMS will reduce the overshoot and undershoot magnitude and the duration. It will help in the DC-link voltage to reach steady-state quicker.

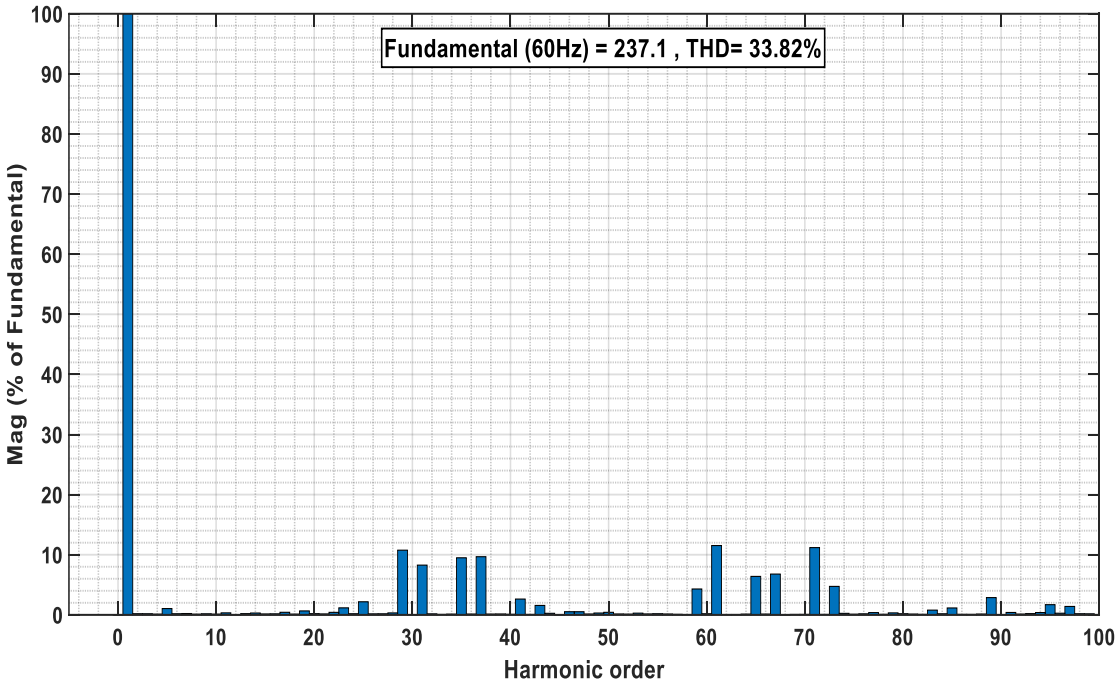

Figure 4.8. Converter output voltage without filtration for PV microgrid

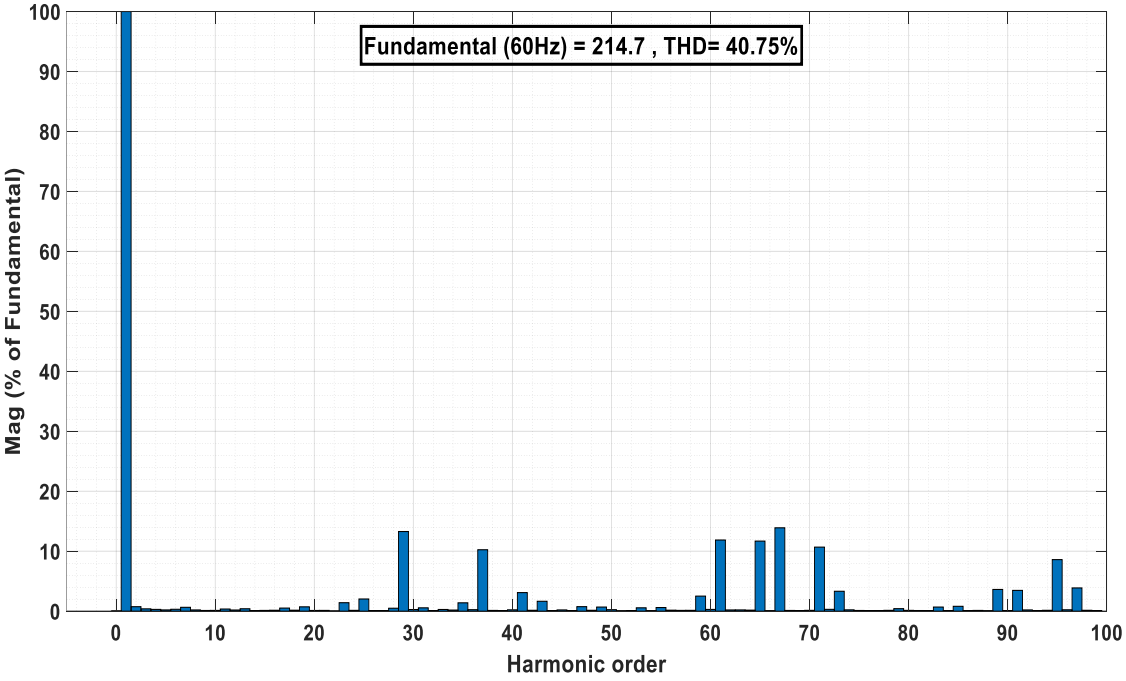

Figure 4.9. Converter output voltage without filtration for PV-battery microgrid

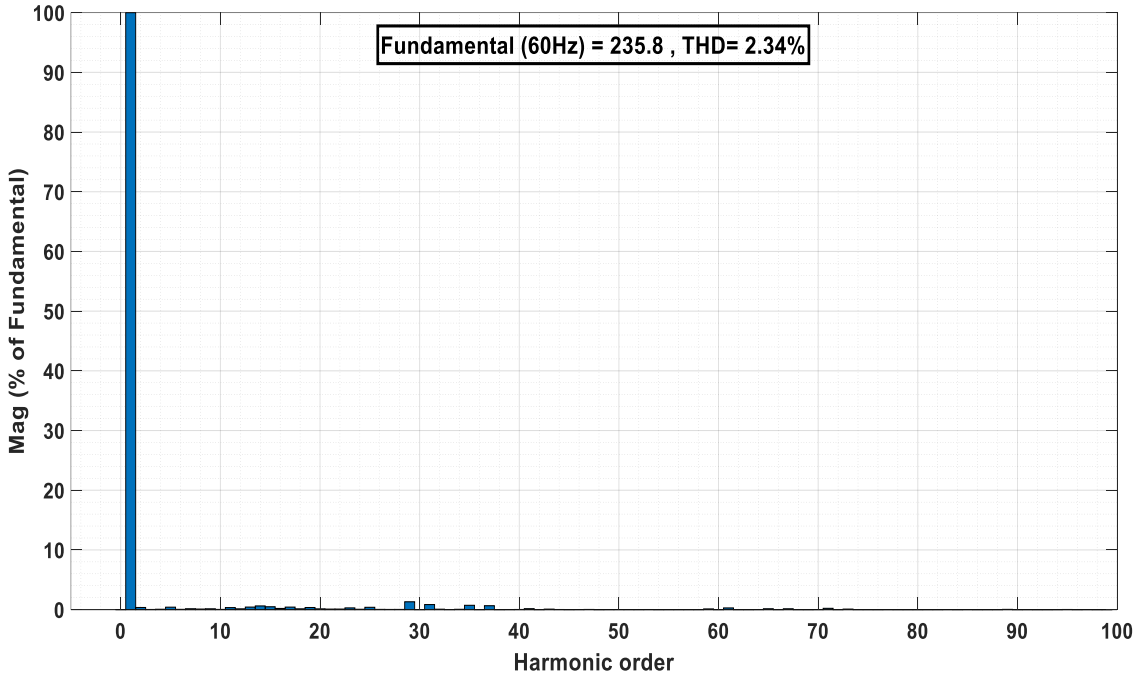

Figure 4.10. Converter output voltage without filtration for PV-battery microgrid

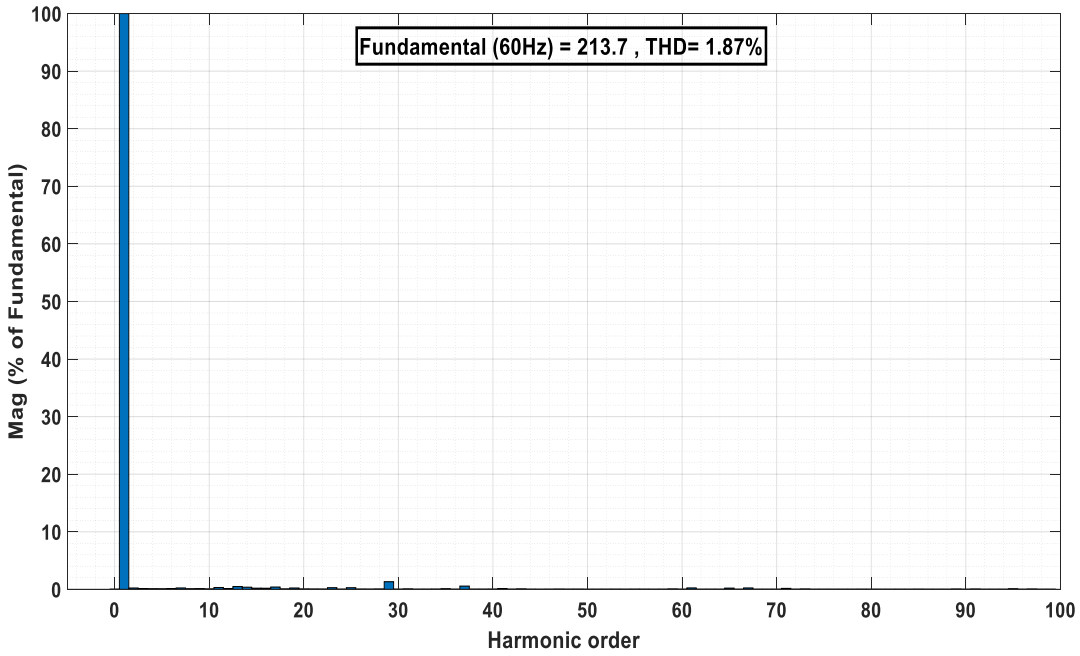

Figure 4.11. Converter output voltage after filtration for PV-battery microgrid

Apart from reducing the harmonics, the battery integration also helps in the compensation of reactive power delivered to the grid. So, the reactive power profile for both cases also need to be discussed. Figure 4.13 shows the reactive power delivered to the grid for both cases. From the graphs, it can be observed that after battery integration the reactive power delivered to the grid reduces. The overall reactive power delivered to the grid is lower for PV-battery microgrid. The reactive power is only developed in case of voltage unbalance which is expected as mentioned in the section 3.

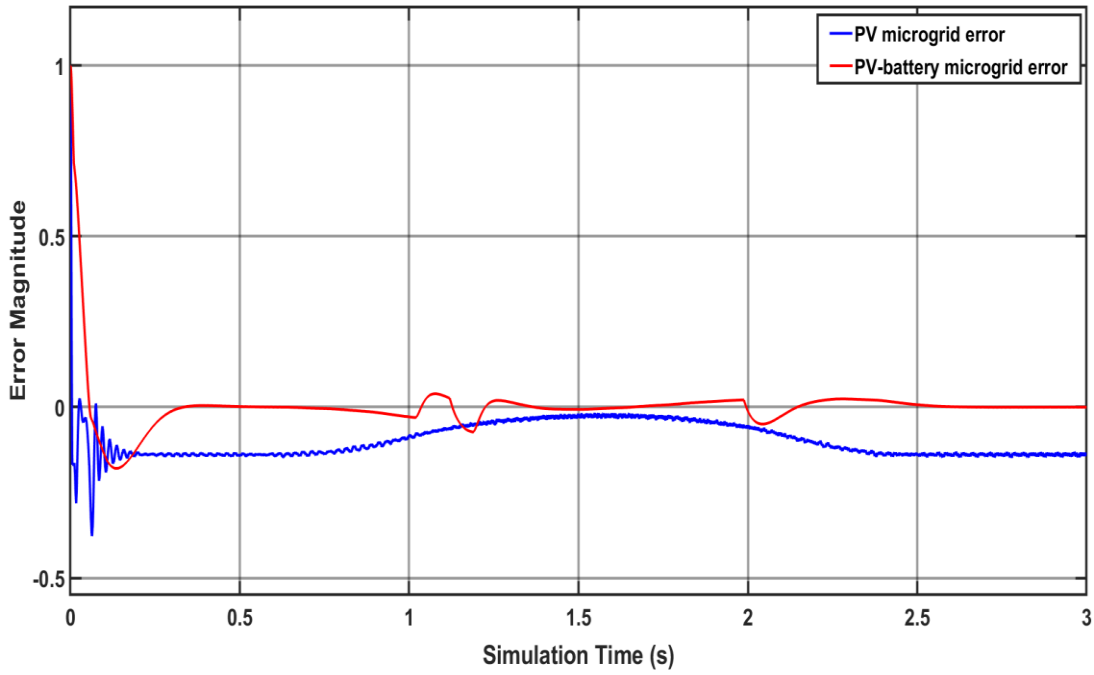

Figure 4.12. DC-link voltage error for PV and PV-battery microgrid

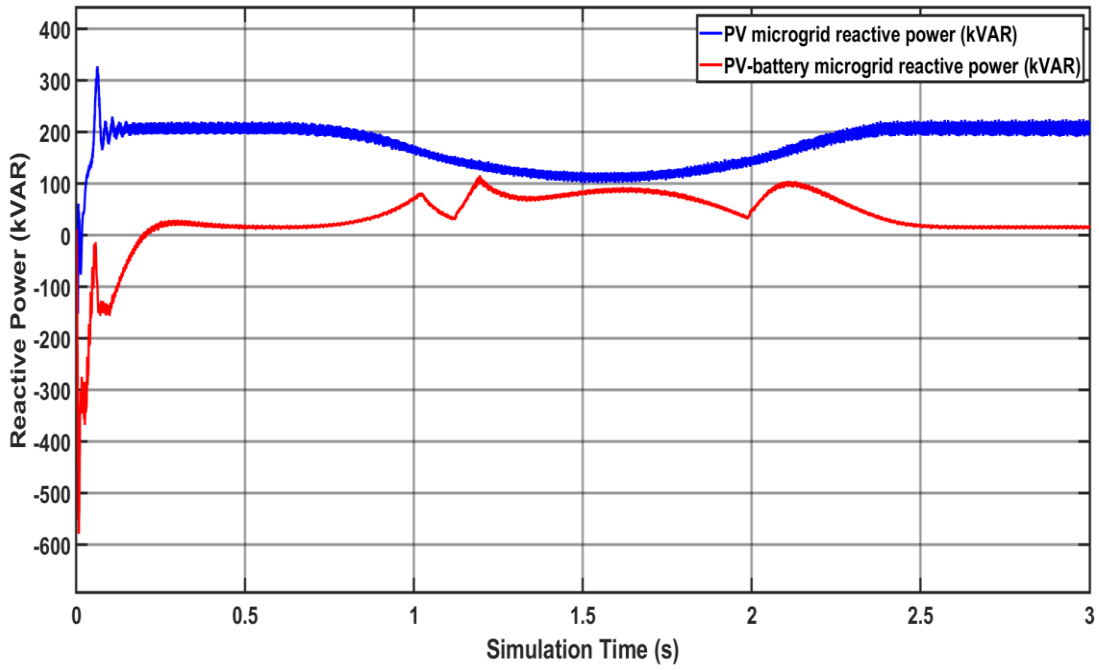

Figure 4.13. Reactive power of PV and PV-battery microgrid

From the results mentioned above, it can be seen that battery paired with the proposed IFC control can help in mitigating the harmonics while keeping the voltage at the required levels. To have a better comparative analysis, the same system is run using a generic IFC control algorithm. The generic IFC control is a simple voltage comparator without any harmonic compensator. Figure 4.14 and 4.15 shows the THD during simulation time for PV and PV-battery microgrid using generic IFC control, respectively. Figure 4.16 and 4.17 shows the THD during simulation time for PV and PV-battery microgrid using proposed IFC control, respectively. For better illustration, the magnitude of harmonics are also tabulated in Table 4.2.

From the figures and the table, following assessment can be made:

- The DC-link voltage gets effected during the switching of the charging states of the battery.
- The presence of harmonic compensator in the IFC control helps in the mitigation of the harmonics.

- The THD for the generic IFC control for both, the PV and PV-battery case is higher when compared to the proposed IFC control strategy.
- Integration of battery with the IFC control helps in the mitigation of the lower order harmonics.
- High order harmonics are increased due to the DC-link voltage unbalance due to the charging and discharging of the battery.

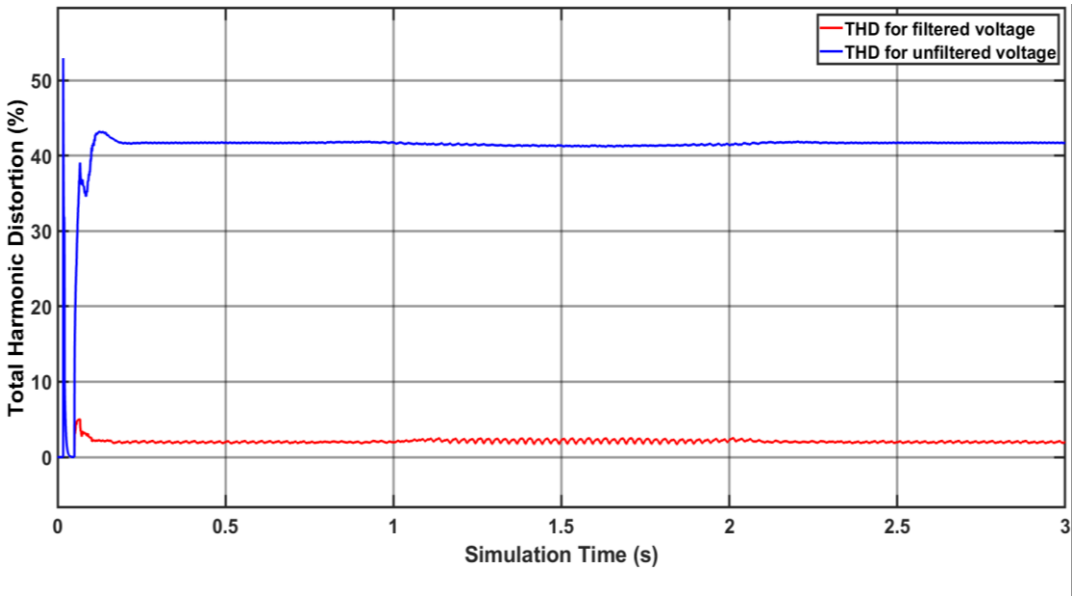

Figure 4.14. THD for PV microgrid using generic IFC control

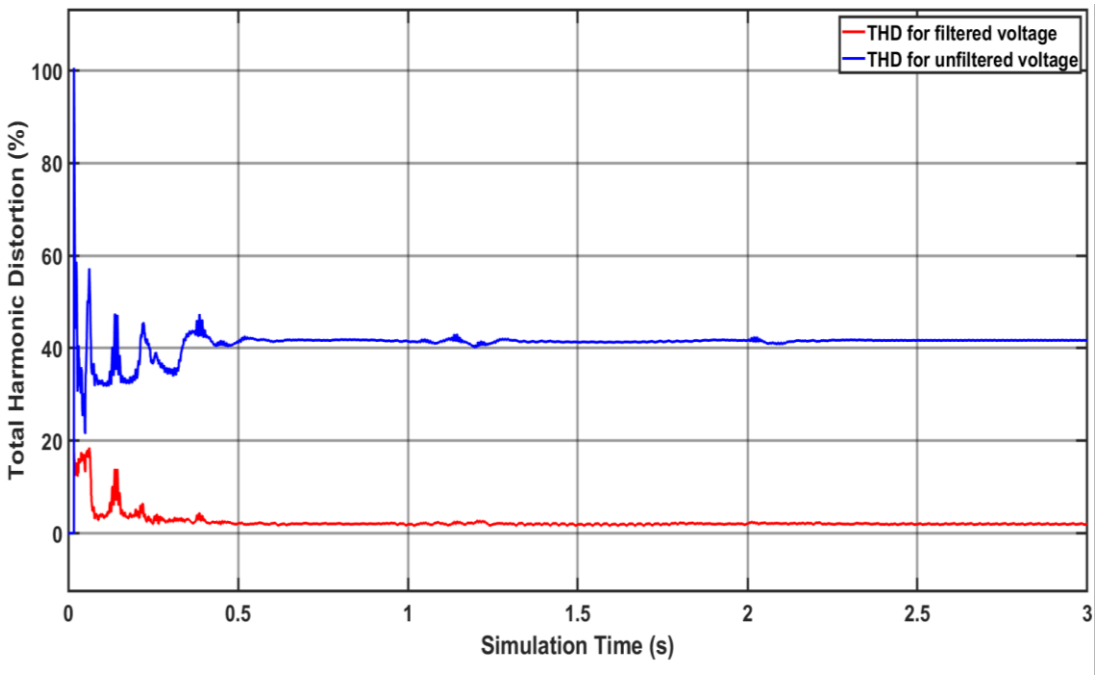

Figure 4.15. THD for PV-battery microgrid using generic IFC control

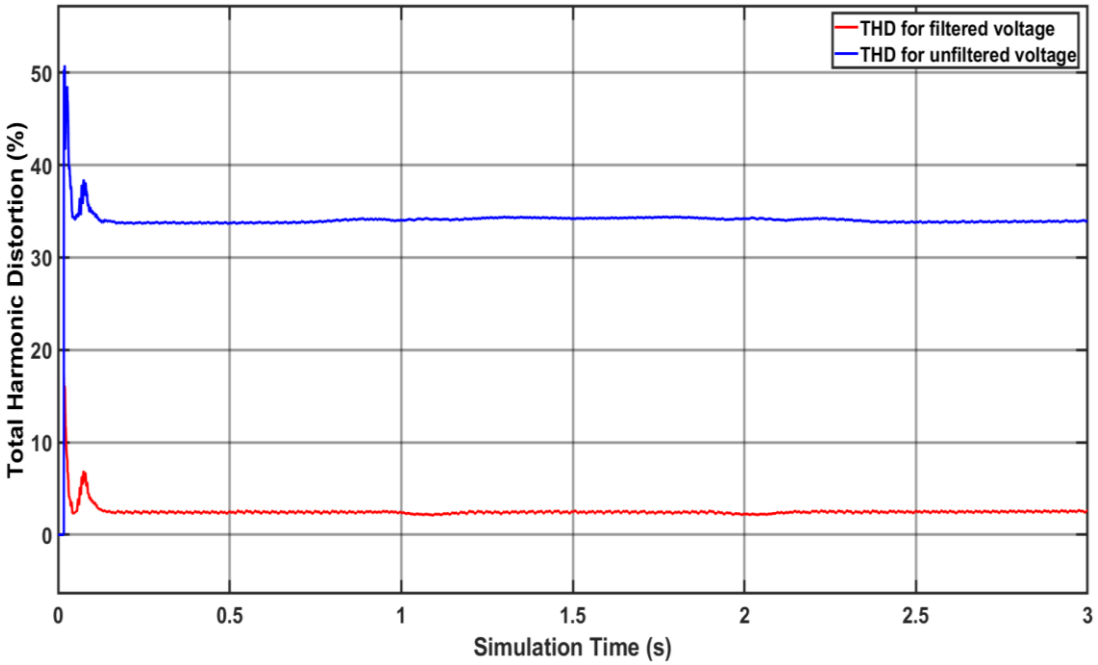

Figure 4.16. THD for PV microgrid using proposed IFC control

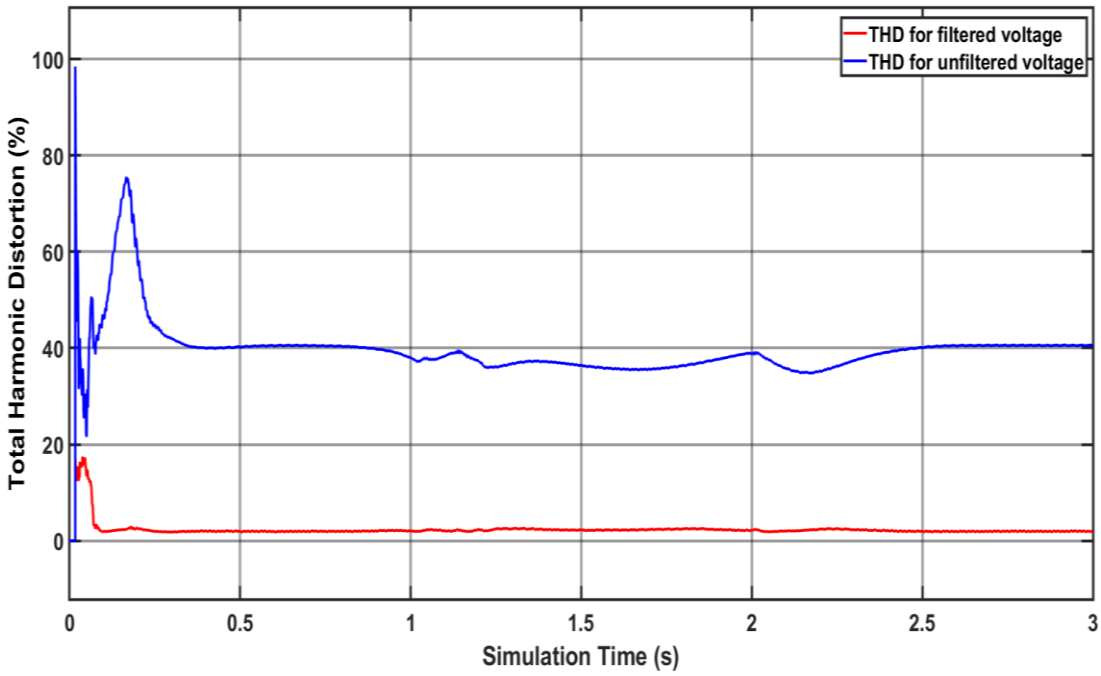

Figure 4.17. THD for PV-battery microgrid using proposed IFC control

Table 4.2. Magnitude of Harmonics for PV and PV-battery microgrids using generic IFC control and proposed IFC control

Magnitude of Harmonics								
	Generic IFC control (PV)		Generic IFC control (PV-battery)		Proposed IFC control (PV-battery)		Proposed IFC control (PV-battery)	
Harmonic order	Without filtration THD= 41.9%	After filtration THD= 2.9%	Without filtration THD= 43.7%	After filtration THD= 2.3%	Without filtration THD= 33.8%	After filtration THD= 2.3%	Without filtration THD= 40.7%	After filtration THD= 1.8%
5^{th}	1.04%	0.41%	0.29%	0.13%	1.04%	0.41%	0.13%	0.06%
7^{th}	0.66%	0.25%	0.11%	0.04%	0.22%	0.14%	0.17%	0.10%
11^{th}	0.29%	0.27%	0.29%	0.24%	0.31%	0.34%	0.39%	0.26%
13^{th}	0.27%	0.25%	1.26%	0.74%	0.20%	0.42%	0.41%	0.29%
17^{th}	0.24%	0.21%	0.54%	0.44%	0.45%	0.42%	0.81%	0.42%
19^{th}	0.45%	0.15%	0.63%	0.23%	0.71%	0.35%	0.97%	0.23%

CHAPTER 5

CONCLUSION

Integration of RES as DG into the microgrid has increased over the last decade. RES being a variable source, produce variable power. To ensure constant power supply to the grid and the load, IFC are used. But the use of IFC gives rise to harmonics at the output. Also, the increased usage of non-linear loads, can cause harmonics. One more issue with RES, is the waste of the excess power. Hence, ESS can be useful as they allow the storage of excess power. ESS can also be used for power quality improvement and harmonic mitigation. However, in the literature, there is few research available which discuss the power quality conditioning capabilities of ESS. And even if they discuss it, they do not present comparative analysis.

A PV-battery system is modelled in this study. The irradiation and the demand data is used of our university, METU NCC. A voltage controller paired with a RSC is used to control the IFC gating signals. Voltage controller ensures that the DC-link voltage is kept at the reference voltage and reactive power is compensated. RSC is used for this study because RSC allows to selective harmonic compensation by setting the resonant frequency as the frequency which needs to be removed. A impedance compensator is also present in the IFC control to take leakage and shunt impedance of the transformer into account. The algorithm for the BMS is simple. When the power from PV exceeds the demand, the excess power is stored in the battery. Otherwise, the battery supplies power to the grid.

First, the PV-battery is simulated to verify the validity of system. The PV power delivered is compared with the theoretically estimated power. The power obtained from our model is similar to the expected power apart from a little loss which is expected as in the theoretical calculation, the losses due to temperature and external factors are excluded. The SOC and the DC-link voltage plots confirm the overall working of the IFC and BMS. The voltages obtained at the output before and after filtration are also as expected. Before filtration, the voltage is squarer shaped due to

presence of high order harmonics. After filtration, the voltage becomes smoother and becomes a sine wave.

For harmonic analysis, THD calculation is required. THD is obtained through Fourier transform. To show the effect of battery on the harmonics of the system, the THD for a PV-battery system is compared with the THD of a battery system. The comparisons shows that the THD for unfiltered voltage for PV-battery microgrid is 40.75% which greater than the THD for PV microgrid which is 33.82%. After filtration the THD for PV-battery microgrid is 1.87% while for the PV microgrid it is 2.34%. These results show that integrating battery into the system increases the high order harmonics due to unbalanced caused in the DC-link voltage during the switching of the charging modes. After filtration, the THD for PV-battery microgrid is lower than the PV-microgrid. This shows that the integration of battery into the microgrid helps the IFC to filter out the low order harmonics. This is expected as the integration of battery provides an extra voltage source to stabilize the DC-link voltage. This is shown by the error plots in the reference voltage generator. The error between the reference DC-link voltage and instantaneous DC-link voltage for PV-battery microgrid is less when compared to the error for PV microgrid. The overall change is THD during the course of simulation for PV-battery and PV microgrid is shown in appendix C which verifies our results.

The effect of battery on the reactive power developed at the grid is also discussed as it is also an important power quality concern. The comparison of reactive power shows that the reactive power developed for PV-battery is lower compared to the PV microgrid. The reactive power for the PV microgrid is generally higher and only decreases during charging of the battery. For the PV-battery microgrid, the reactive power developed during the steady state is generally lower but due to the unbalance of the DC-link voltage during charging and discharging, increases the reactive power which is expected. One thing that needs to mentioned is that the unbalance in the DC-link voltage can be improved further by designing a more complex and efficient BMS. The improved BMS would reduce the unbalance and allow the system to reach the steady state even faster.

This study verifies the effect of integrating battery into the microgrid on the power quality. In the literature review, it is mentioned there are very few studies available in the literature which comprehensively go over the effect of ESS on the power quality. Also, few studies are available which discuss the IFC control design for a ESS integrated microgrid. This study contains step by step approach to designing a PV-battery system which can help the reader in their design. This study shows that ESS can be used not only to improve the RES fraction of a microgrid but can also be used to improve the power quality delivered. This will encourage the system designers to integrate for ESS into the microgrids and move towards a more sustainable future.

REFERENCES

[1] S. Khan, B. Singh, and P. Makhija, "A review on power quality problems and its improvement techniques," *2017 Innov. Power Adv. Comput. Technol. i-PACT 2017*, vol. 2017-Janua, pp. 1–7, 2017, doi: 10.1109/IPACT.2017.8244882.

[2] G. N. Popa, A. Iagăr, and C. M. Diniș, "Considerations on current and voltage unbalance of nonlinear loads in residential and educational sectors," *Energies*, vol. 14, no. 1, 2021, doi: 10.3390/en14010102.

[3] C. R. Bayliss and B. J. Hardy, "Power Quality – Voltage Disturbances," in *Transmission and Distribution Electrical Engineering*, Newnes, 2012, pp. 1013–1026.

[4] F. Nejabatkhah, Y. W. Li, and H. Tian, "Power quality control of smart hybrid AC/DC microgrids: An overview," *IEEE Access*, vol. 7, pp. 52295–52318, 2019, doi: 10.1109/ACCESS.2019.2912376.

[5] Pinyol Ramon, "Harmonics : Causes , Effects and Minimization," *Salicru White Pap.*, no. August, pp. 1–32, 2015.

[6] C. K. Duffey and R. P. Stratford, "Update of harmonic standard IEEE-519 - IEEE Recommended Practices and Requirements for Harmonic Control in Electric Power Systems," *Conf. Rec. - IAS Annu. Meet. (IEEE Ind. Appl. Soc.*, no. pt 2, pp. 1618–1624, 1989, doi: 10.1109/PCICON.1988.22445.

[7] F. Nejabatkhah, Y. Li, and B. Wu, "Control strategies of three-phase distributed generation inverters for grid unbalanced voltage compensation," in *2015 IEEE Energy Conversion Congress and Exposition, ECCE 2015*, Oct. 2015, pp. 6467–6474, doi: 10.1109/ECCE.2015.7310566.

[8] A. Camacho, M. Castilla, J. Miret, J. C. Vasquez, and E. Alarcon-Gallo, "Flexible voltage support control for three-phase distributed generation inverters under grid fault," *IEEE Trans. Ind. Electron.*, vol. 60, no. 4, pp. 1429–1441, 2013, doi: 10.1109/TIE.2012.2185016.

[9] C. T. Lee, C. W. Hsu, and P. T. Cheng, "A low-voltage ride-through technique for grid-connected converters of distributed energy resources," *IEEE Trans. Ind. Appl.*, vol. 47, no. 4, pp. 1821–1832, Jul. 2011, doi: 10.1109/TIA.2011.2155016.

[10] J. Miret, M. Castilla, A. Camacho, L. G. De Vicuña, and J. Matas, "Control scheme for photovoltaic three-phase inverters to minimize peak currents during unbalanced grid-voltage sags," *IEEE Trans. Power Electron.*, vol. 27, no. 10, pp. 4262–4271, 2012, doi: 10.1109/TPEL.2012.2191306.

[11] A. Camacho, M. Castilla, J. Miret, A. Borrell, and L. G. De Vicuña, "Active and reactive power strategies with peak current limitation for distributed

generation inverters during unbalanced grid faults," *IEEE Trans. Ind. Electron.*, vol. 62, no. 3, pp. 1515–1525, Mar. 2015, doi: 10.1109/TIE.2014.2347266.

[12] J. Lu, F. Nejabatkhah, Y. Li, and B. Wu, "DG control strategies for grid voltage unbalance compensation," *2014 IEEE Energy Convers. Congr. Expo. ECCE 2014*, pp. 2932–2939, Nov. 2014, doi: 10.1109/ECCE.2014.6953797.

[13] S. K. Chaudhary, R. Teodorescu, P. Rodriguez, P. C. Kjaer, and A. M. Gole, "Negative sequence current control in wind power plants with VSC-HVDC connection," *IEEE Trans. Sustain. Energy*, vol. 3, no. 3, pp. 535–544, 2012, doi: 10.1109/TSTE.2012.2191581.

[14] D. Salles, C. Jiang, W. Xu, W. Freitas, and H. E. Mazin, "Assessing the collective harmonic impact of modern residential loads-part I: Methodology," *IEEE Trans. Power Deliv.*, vol. 27, no. 4, pp. 1937–1946, 2012, doi: 10.1109/TPWRD.2012.2207132.

[15] J. Zhang, L. Li, D. G. Dorrell, and Y. Guo, "Space vector modulation based proportional resonant current controller with selective harmonics compensation for matrix converter systems," *2017 20th Int. Conf. Electr. Mach. Syst. ICEMS 2017*, no. August, 2017, doi: 10.1109/ICEMS.2017.8055959.

[16] Z. Xin, P. Mattavelli, W. Yao, Y. Yang, F. Blaabjerg, and P. C. Loh, "Mitigation of Grid-Current Distortion for LCL-Filtered Voltage-Source Inverter with Inverter-Current Feedback Control," *IEEE Trans. Power Electron.*, vol. 33, no. 7, pp. 6248–6261, Jul. 2018, doi: 10.1109/TPEL.2017.2740946.

[17] D. De and V. Ramanarayanan, "A proportional + multiresonant controller for three-phase four-wire high-frequency link inverter," *IEEE Trans. Power Electron.*, vol. 25, no. 4, pp. 899–906, 2010, doi: 10.1109/TPEL.2009.2036012.

[18] T. L. Lee and S. H. Hu, "An Active Filter with Resonant Current Control to Suppress Harmonic Resonance in a Distribution Power System," *IEEE J. Emerg. Sel. Top. Power Electron.*, vol. 4, no. 1, pp. 198–209, Mar. 2016, doi: 10.1109/JESTPE.2015.2478149.

[19] Y. Yang, K. Zhou, H. Wang, and F. Blaabjerg, "Harmonics mitigation of dead time effects in PWM converters using a repetitive controller," *Conf. Proc. - IEEE Appl. Power Electron. Conf. Expo. - APEC*, vol. 2015-May, no. May, pp. 1479–1486, May 2015, doi: 10.1109/APEC.2015.7104543.

[20] R. Costa-Castelló, R. Grinó, and E. Fossas, "Odd-harmonic digital repetitive control of a single-phase current active filter," *IEEE Trans. Power Electron.*, vol. 19, no. 4, pp. 1060–1068, 2004, doi: 10.1109/TPEL.2004.830045.

[21] G. Escobar, P. R. Martínez, J. Leyva-Ramos, and P. Mattavelli, "A negative feedback repetitive control scheme for harmonic compensation," *IEEE Trans. Ind. Electron.*, vol. 53, no. 4, pp. 1383–1386, Jun. 2006, doi: 10.1109/TIE.2006.878293.

[22] K. Zhou, Y. Yang, F. Blaabjerg, and D. Wang, “Optimal selective harmonic control for power harmonics mitigation,” *IEEE Trans. Ind. Electron.*, vol. 62, no. 2, pp. 1220–1230, Feb. 2015, doi: 10.1109/TIE.2014.2336629.

[23] S. Buso, T. Caldognetto, and D. I. Brandao, “Dead-beat current controller for voltage source converters with improved large-signal response,” *IEEE Trans. Ind. Appl.*, vol. 2015, pp. 1588–1596, 2015, doi: 10.1109/TIA.2015.2488644.

[24] A. Kulkarni and V. John, “Mitigation of lower order harmonics in a grid-connected single-phase PV inverter,” *IEEE Trans. Power Electron.*, vol. 28, no. 11, pp. 5024–5037, 2013, doi: 10.1109/TPEL.2013.2238557.

[25] L. Al-Ghussain, R. Samu, O. Taylan, and M. Fahrioglu, “Sizing renewable energy systems with energy storage systems in microgrids for maximum cost-efficient utilization of renewable energy resources,” *Sustain. Cities Soc.*, vol. 55, p. 102059, Apr. 2020, doi: 10.1016/J.SCS.2020.102059.

[26] S. M. S. Sadati, E. Jahani, O. Taylan, and D. K. Baker, “Sizing of Photovoltaic-Wind-Battery Hybrid System for a Mediterranean Island Community Based on Estimated and Measured Meteorological Data,” *J. Sol. Energy Eng. Trans. ASME*, vol. 140, no. 1, Feb. 2018, doi: 10.1115/1.4038466.

[27] G. Panayiotou, S. Kalogirou, and S. Tassou, “Design and simulation of a PV and a PV–Wind standalone energy system to power a household application,” *Renew. Energy*, vol. 37, no. 1, pp. 355–363, Jan. 2012, doi: 10.1016/J.RENENE.2011.06.038.

[28] S. Diaf, D. Diaf, M. Belhamel, M. Haddadi, and A. Louche, “A methodology for optimal sizing of autonomous hybrid PV/wind system,” *Energy Policy*, vol. 35, no. 11, pp. 5708–5718, Nov. 2007, doi: 10.1016/J.ENPOL.2007.06.020.

[29] G. Liu, M. G. Rasul, M. T. O. Amanullah, and M. M. K. Khan, “Feasibility study of stand-alone PV-wind-biomass hybrid energy system in Australia,” *Asia-Pacific Power Energy Eng. Conf. APPEEC*, 2011, doi: 10.1109/APPEEC.2011.5749125.

[30] L. Deotti, W. Guedes, B. Dias, and T. Soares, “Technical and Economic Analysis of Battery Storage for Residential Solar Photovoltaic Systems in the Brazilian Regulatory Context,” *Energies 2020, Vol. 13, Page 6517*, vol. 13, no. 24, p. 6517, Dec. 2020, doi: 10.3390/EN13246517.

[31] L. Xu, Z. Miao, L. Fan, and G. Gurlaskie, “Unbalance and harmonic mitigation using battery inverters,” *2015 North Am. Power Symp. NAPS 2015*, Nov. 2015, doi: 10.1109/NAPS.2015.7335119.

[32] J. Zeng, B. Zhang, C. Mao, and Y. Wang, “Use of battery energy storage system to improve the power quality and stability of wind farms,” *2006 Int. Conf. Power Syst. Technol. POWERCON2006*, 2006, doi: 10.1109/ICPST.2006.321662.

[33] J. A. Mundackal, A. C. Varghese, P. Sreekala, and V. Reshmi, “Grid power quality improvement and battery energy storage in wind energy systems,” *2013 Annu. Int. Conf. Emerg. Res. Areas, AICERA 2013 2013 Int. Conf. Microelectron. Commun. Renew. Energy, ICMiCR 2013 - Proc.*, 2013, doi: 10.1109/AICERA-ICMICR.2013.6576010.

[34] S. M. Muyeen, R. Takahashi, T. Murata, J. Tamura, and M. H. Ali, “Application of STATCOM/BESS for wind power smoothening and hydrogen generation,” *Electr. Power Syst. Res.*, vol. 79, no. 2, pp. 365–373, Feb. 2009, doi: 10.1016/J.EPSR.2008.07.007.

[35] S. Kirmani and B. Kumar, “Power quality improvement by using STATCOM control scheme in wind energy generation interface to grid,” *IOP Conf. Ser. Earth Environ. Sci.*, vol. 114, no. 1, p. 012001, Jan. 2018, doi: 10.1088/1755-1315/114/1/012001.

[36] J. M. Guerrero, P. C. Loh, T. L. Lee, and M. Chandorkar, “Advanced control architectures for intelligent microgridsPart II: Power quality, energy storage, and AC/DC microgrids,” *IEEE Trans. Ind. Electron.*, vol. 60, no. 4, pp. 1263–1270, 2013, doi: 10.1109/TIE.2012.2196889.

[37] M. Ovaskainen, J. Öörni, and A. Leinonen, “Superposed control strategies of a BESS for power exchange and microgrid power quality improvement,” *Proc. - 2019 IEEE Int. Conf. Environ. Electr. Eng. 2019 IEEE Ind. Commer. Power Syst. Eur. EEEIC/I CPS Eur. 2019*, Jun. 2019, doi: 10.1109/EEEIC.2019.8783764.

[38] J. A. Duffie, W. A. Beckman, and J. McGowan, “Solar Engineering of Thermal Processes,” *Am. J. Phys.*, vol. 53, no. 4, pp. 382–382, 1985, doi: 10.1119/1.14178.

[39] “Axitec 60 cell polycrystalline photovoltaic modules İngilizce | Manualzz.” https://manualzz.com/doc/9569919/axitec-60-cell-polycrystalline-photovoltaic-modules-ingi... (accessed Aug. 01, 2021).

[40] D. Lu, X. Wang, and F. Blaabjerg, “Influence of Reactive Power Flow on the DC-Link Voltage Control in Voltage-Source Converters,” *2018 IEEE Energy Convers. Congr. Expo. ECCE 2018*, pp. 2236–2241, Dec. 2018, doi: 10.1109/ECCE.2018.8557485.

APPENDICES

A. Switching time of the boost converter

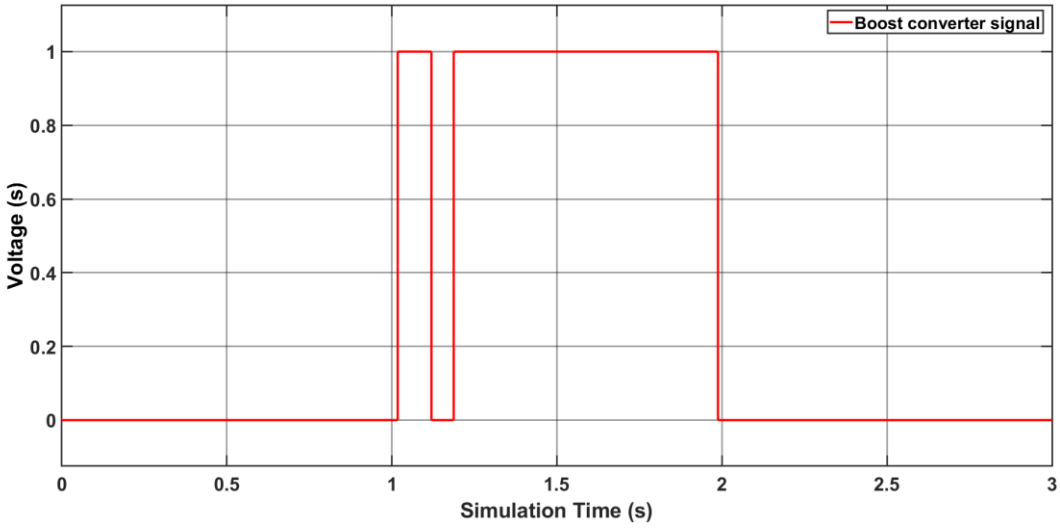

Figure A.1. ON signal for the boost converter connected to battery

B. THD for harmonics of both cases

Table B.1. Magnitude of fundamental frequency for proposed IFC control for PV and PV-battery microgrid

	% Of magnitude of fundamental frequency			
Harmonic Order	Without battery unfiltered	Without battery filtered	With battery unfiltered	With battery filtered
3rd	0.06%	0.02%	0.46%	0.16%
5th	1.04%	0.41%	0.13%	0.06%
7th	0.22%	0.14%	0.17%	0.10%
9th	0.14%	0.13%	0.06%	0.08%
11th	0.24%	0.34%	0.39%	0.26%
13th	0.20%	0.42%	0.41%	0.29%
15th	0.15%	0.48%	0.15%	0.30%
17th	0.45%	0.42%	0.81%	0.42%
19th	0.71%	0.35%	0.97%	0.23%
21st	0.17%	0.08%	0.18%	0.03%
23rd	1.16%	0.29%	1.39%	0.28%
25th	2.12%	0.39%	2.04%	0.28%
27th	0.20%	0.03%	0.17%	0.02%
29th	10.77%	1.31%	13.24%	1.33%
31st	8.29%	0.85%	0.44%	0.05%
33rd	0.09%	0.01%	0.26%	0.02%
35th	9.49%	0.72%	1.14%	0.08%
37th	9.61%	0.66%	10.16%	0.56%
39th	0.12%	0.02%	0.11%	0.02%
41st	2.64%	0.15%	3.04%	0.14%
43rd	1.53%	0.07%	1.68%	0.06%

C. System parameters

Table C.1. System parameters

Controller	Parameter for PV
Grid	2500 MVA, 120 kV
PV system	200kW
Inverter side transformer	260V/25kV
Grid side transformer	25kV/120kV
DC-link capacitors	120µF
Battery	50kWh